ELSEVIER

Advanced materials of printed wearables for physiological parameter monitoring

Sithara P. Sreenilayam [1], Inam Ul Ahad [1], Valeria Nicolosi [2], Victor Acinas Garzon [3], Dermot Brabazon [1,*]

[1] I-Form, Advanced Manufacturing Research Centre, & Advanced Processing Technology Research Centre, School of Mechanical and Manufacturing Engineering, Dublin City University, Glasnevin, Dublin 9, Ireland
[2] I-Form and AMBER Research Centers, School of Chemistry, Trinity College Dublin, Dublin 2, Ireland
[3] Applied Materials Ireland Limited, Block A Maynooth Business Campus, Maynooth, Co. Kildare, Ireland

The consumer demand for flexible wearables has increased rapidly with the advent of recent commercial health monitoring systems. The progress in wearable electronics for monitoring physiological parameters in the healthcare industry is rapid and its adaptation is having a positive impact on society. Physiological parameters are important health indicators and their monitoring could effectively enable early detection of disease. This would also help reduce the number of more severe health problems, in disease prevention and lower the overall public sector health cost. Clinical devices for measurement of these parameters are also traditionally non-wearable. Therefore, companies and researchers are focused on the development of new materials and related manufacturing methods which will enable specific wearable health sensors with a high degree of robustness, repeatability and accuracy. On the development of printed physiological signal monitoring devices, much progress has been achieved in recent years. Eventhough several reviews have been presented on flexible and wearable electronics, a detailed summary of the recent progresses on the specific class of printed physiological signal monitoring sensing devices has not been reported. In this review, recent progress and challenges on the functional inks and substrate materials for mass scale production and customization of printed flexible and wearable physiological signal monitoring sensor devices are summarized.

Introduction

Wearable electronics technology is one of the most significant recent innovations which is gradually becoming ubiquitous [1–21]. A tremendous increase in the wearables usage for many application areas has been reported, particularly over the last decade (Fig. 1). These provide many opportunities to overcome demanding key challenges in the society by giving solutions in the field of health care and wellbeing, work safety, enhancement of productivity, energy management of workplaces and homes. The sensing principles of currently available wearable sensing platforms are, capacitive [22–35], resistive [14,36–41] inductive [42], amperometric [43], triboelectric [44–52], voltametric [53], impedance [54], thermoelectric [55], piezoresistive [39,56–68] piezoelectric [69–82], photoelectric [83], pyroelectric [69,70,84–86], resonant [87] and optical [88]. Wearable technologies employed in the healthcare sector for monitoring physiological parameters include body temperature [36,69,89–92], physical pressure [93–99], blood pressure [28,29,62,100,101], respiratory rate [102–104], humidity [105], heart rate (HR) [39,106–108], skin conductance [109] and body movements [110–113]. All of these sensors have their own working principles. For example, flexible temperature sensors developed with metallic tracks printed on polymer substrates typically rely on the variation of

* Corresponding author.
E-mail address: Brabazon, D. (dermot.brabazon@dcu.ie)

https://doi.org/10.1016/j.mattod.2019.08.005

FIGURE 1

Application areas of wearables.

metal resistance with temperature; and the pressure sensor commonly operates via the resistance changing when pressure is applied. The scale and manner of resistance variation is dependent on the materials used for the sensor fabrication.

According to the STOA (European Parliament Scientific & Technology Options Assessment Panel), wearables was identified as one of the number one technologies which will alter society [114]. An advanced truly individualized healthcare system and disease prevention mechanisms is necessary in the world based on a thorough examination of health and disease conditions of the individuals. Over the past couple of years, disease prevention is getting much attention as this treat an individual to prevent a particular disease from occurring [115,116]. In this endeavor, wearable devices, that brought computing and communication much closer to the human body skin, (*e.g.*, shirts [117], necklaces [118], headbands [119], wristbands [120] watches [121], shoes [122], and eyeglasses [123]) are becoming increasingly important for developing human interfaces for motion capture, health monitoring, and disease diagnostics [4,5,12,124–130]. Wearable sensors are the more approapriate devices for the non invasive real time and continuous monitoring of physiological parameters in non-clinical situations when compared to the conventional non-invasive techniques (X-ray, NMR (nuclear magnetic resonance) and type-B ultrasonic) [12,131].

In recent years, flexible devices equipped with wireless connectivity to mobile technologies has stimulated robust growth for wearable device technology. The ability to wirelessly transmit sensed data from a wearable sensor to the external devices enables coupling with a myriad of applications that provide automated feedback to improve user behavior. This presents a strong driver in the market for wireless flexible monitoring devices. The flexible electronics market represents a broad and diverse offering of commercial products. This global market is expected to grow from $ 30 billion US dollars to over $73 billion by 2027 [132]. The advanced vision is the integration of sensor components with computing devices to develop smart, responsive, and intelligent systems for prosthetics and humanoid technologies [133,134], which include synaptic devices for signal processing, skin like materials for substrate engineering, and bioinspired patterns in sensor devices for improving signal transduction [108,135–141]. Ever evolving advances in sensing materials, manufacturing methods, and sensing techniques have fueled a myriad of developments in the area of flexible sensor technology [648–650]. The unique characteristics of flexible electronics technology will have an enormous beneficial impact for wearables due to their characteristics such as compliant structures, ultra-thin profiles, lightweight, potential for low cost and high reliability.

The wearable sector is considered to have reached a stage where it needs to go in a new direction for fulfilling the huge potential it has in the digital society of the future. The future directions for research are toward developing low cost smart wearables made up of printed high quality electronic devices for a long term contribution to the digital healthcare. The sensed data obtained by the smart wearables is processed and the results are ultimately provided to the wearer. There are still a number of hurdles to cross before the technology reaches the maturity required for larger-scale commercial roll-out. Often wearables do not record sufficient data for producing enough details to the clinician or researcher. Smart wearable must be stable and widely available, should cost as little as possible, and work reliably. If the problems associated with the currently available wearable health devices are overcome, the use of wearables to measure physical outcomes and monitor patients would make them an invaluable tool in clinical trials.

Very recently, a number of review articles have been reported on the flexibe and wearable electronics, flexible batteries and functional inks. However, a detailed summary of materials and methods for printed physiological parameter moniting devices has not been reported. This area is of significant research interest as revealed by the increasing research efforts and advancements. Therefore, this review article specifically summarizes the state-of-art research progress on high performance sensing materials, storage devices and printing technologies for large-scale flexible and wearable physiological parameter monitoring sensor devices.

Manufacturing technologies of flexible sensors

The advancement of wearable and flexible sensor devices leads developements in materials science and manufacturing methods. Flexible multifunctional sensors are one of the emerging technologies in wearables which need lower cost, increased reproducibility, increased accuracy, good mechanical stability and high sensitivity [652]. Multiple parameters can be simultaneously detected using these devices. A traditional flexible multifunctional sensor consist of a pizoelectric sensor and other different sensors with separate sensing mechanisms on different substrates [653,654]. In this class of sensors, the piezoelectric effect (providing an electrical resistance variation with applied stress) is combined with other separate sensing mechanisms. Interconnects are used to connect these separate sensors in a particular device. Numerous flexible sensor component and

interconnect fabrication techniques have been demonstrated already [142–157]. In recent years, printing technologies have inceased in popularity for high performance electronic components fabrication and associated sensor devices on flexible substrates at the required processing temperatures [158–160]. An important benefit of printing technology is additivity, as patterns/structures are fabricated by the addition of materials in layer by layer, however traditional manufacturing techniques are based on the subtraction of material causing increased amount of waste production that leads to environmental problems. The additive process will often lower the number of manufacturing steps required on the assembly line, providing a significantly faster production route. The main physical component of Printed Electronics (PE) is the functional ink, that is normally composed of organic and/or inorganic materials [341,644]. This peculiar ink mixture enables the homogenious and perfect deposition of the functional ink over flexible polymer substrates (for example, polyethylene terephthalate (PET), polyimide (PI), polyethlenenaphthalate (PEN), poly carbonate (PC) *etc*.) and followed by high temperature curing of the substrates that are coated with inks. The temperature range for effective curing of the substrates coated with functional silver (Ag) ink is 110 – 350 °C [655–657]. Silver is the most common metallic conductive ink used in the market, and this continues to be the most prominent material in conductive inks, that can be used in many forms such as micron flakes, nanoparticles, organo-metallic formulations and nano wires. This is mainly because its oxide form also conducts and this material therefore has a low technological risk for usage. If the ink conductivity is higher, less ink is also required for device fabrication. Functional ink printing can be carry out using different methods such as inkjet printing, screen printing, and roll-to roll printing techniques [645,646]. The components and devices realized by these printing technologies are discrete electric components (wirings, bus bars, electrodes, resistors, capacitors, inductors, and antennas) [161–163], active electronic devices ((photo-)diodes, transistors, OLEDs [164–168] and solar cells [169]), memory devices (ferroelectric capacitor) [170], energy storage (batteries) [171,172], sensors (physical, and electro chemical) [173–175] and Flexible Hybrid Systems (surface-mount devices (SMDs) and PEs) [176]. Owing to their capability of bypassing conventional electronics based on silicon to manufacture different devices on flexible/stretchable substrates, PE obtained much attraction in the field of electronic components and device manufacturing. The growing applications of nanotechnology in electronics, photonics, and biomedical require manufacturing techniques capable to print nanofeatures at high throughput. Nanoimprint lithography (NIL) enables fabrication of nanodevices with nanometre scale feature size and high aspect ratios.

The flexible wearable device market for self-monitoring health is growing very fast and this printed wearable sensor area has a huge potential. The current capabilities of these devices include physiological and biochemical sensing. The physiological parameters monitoring help to understand the time sensitive state of health as these are released continuously/regularly by individual's engagement level and/or emotional states. A few examples of printed physiological parameters monitoring devices are shown in Fig. 2a.

To advance productive fabrication of electronic components/device, flexographic, screen, inkjet, gravure and 3D printing techniques are being developed prominently (Fig. 2b) [183]. All these methods have their own specific benefits and drawbacks. Therefore, complex devices/systems will probably be manufactured using the incorporation of various printing technologies. These printing methods could be divided into two categories, contact (*e.g*. Screen, Flexography and Gravure) and non-contact printing (*e.g*. Inkjet). Although the contact printing techniques are widely used for large-area printing, non-contact printing technologies provide comparatively higher resolution and enable use of wide range of materials. The manufacturing processes can be implemented in roll-to-roll (R2R) and sheet-to-sheet (S2S) approachess to print monolayer and multilayer devices based on the method of substrate feeding (Fig. 2c and d). R2R is the method of producing PEs on a roll of metal foil or flexible substrates and S2S is the method of producing PEs on a sheet of metal foil or flexible substrates. The main difference between both approaches is feeding of the printing substrate in a roll or sheet format. The S2S process allows printing on area from few square centrimeter to several square meters. However, the substrate velocity is comparatively slow in S2S production which significantly reduces the production speed [184]. The R2R technology exhibits advantages including high process speeds and the additive nature, over traditional methods for high yield manufacturing of parts on flexible and stretchable substrates. This is a classic substrate based printing technique in which additive and subtractive processes can be used to fabricate complex patterns/structures in a continuous manner. This printing technology is very suitable for high-volume and large-scale manufacturing of PE devices.

Flexible electronic circuits fabrication generates many challenges. This involves designing conductive patterns on a flexible substrate, joining electronic parts to the flexible electronics circuit without changing electrical conductivity and sensor interface with outside system for the transmission of power, acquisition of data and conditioning of signal. The essential requirements for wearable electronic devices are their biocompatibility, huge flexibility and durability and should possess lower weight. Hence, when carrying out PE techniques, it is vital to consider (1) the usage of chemically stable and well soluble non-toxic functional inks that can be processable at lower temperature, for easy printing and suitable post treatment (2) production of high resolution uniform patterns for good electrical conductivity and excellent amalgamation of devices, (3) the usage of compatible flexible substrates to integreate with the human body skin, and (4) specific structure of the device design to avoid problems including sliding and cracking for long lasting device performance and use. Introduction of toxicants from consumer electronics without any control has negatively affected on the environment. For example, nickel-cadmium batteries are banned for consumers in the European Union as these batteries contain 18% cadmium, which is a toxic heavy metal [668]. There are also many lead containing electronic consumer products that will also pose environmental health issues [669]. Organic electronics have emerged as an excellent solution to overcome the challenge of biocompatible and production of green flexible electronics [670]. Organic materials can be deposited on substrates

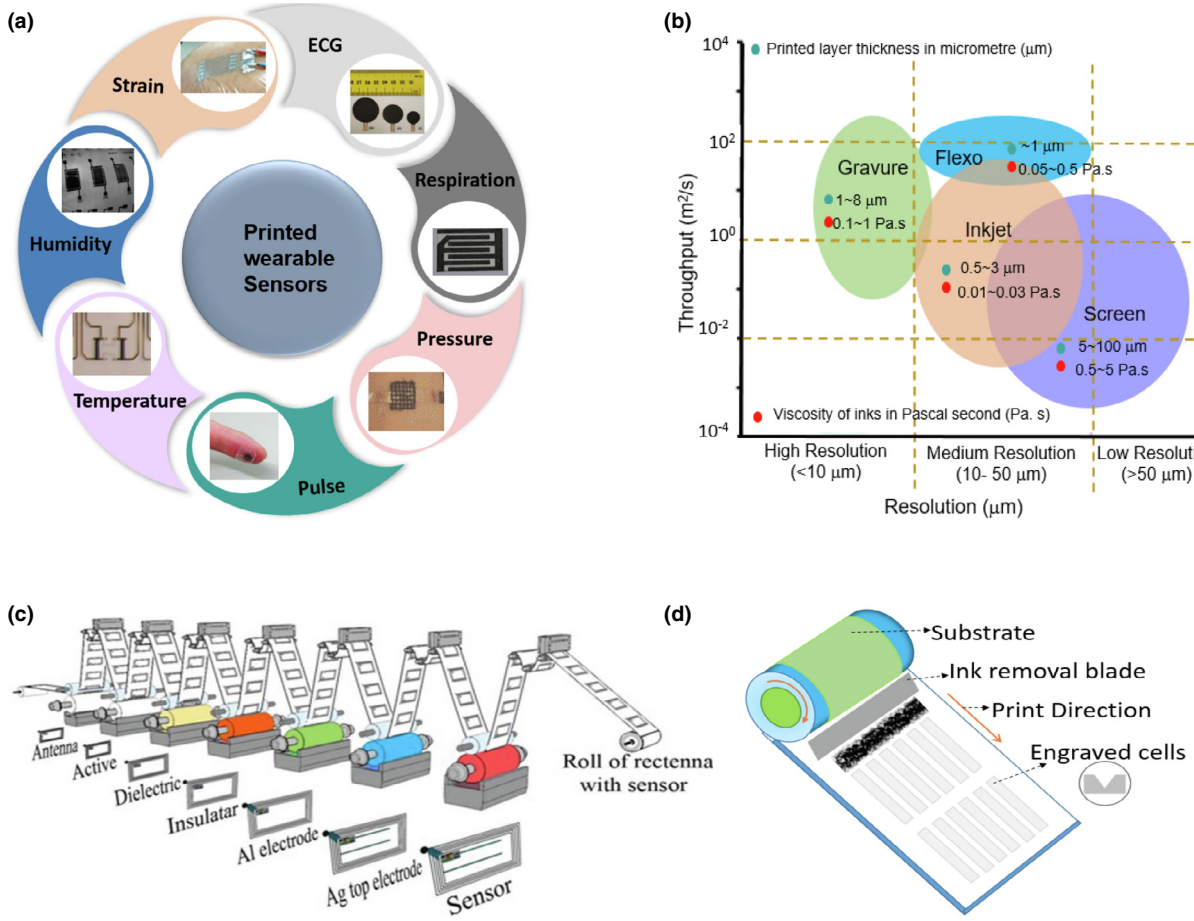

FIGURE 2

Printed sensors and printing technologies. (a) Printed physiological parameters monitoring sensors (ECG (Reprinted from the Ref. [177], Copyright 2018 with permission from Elsevier), Respiration (Reprinted from the Ref. [178], Copyright © 2016 with permission from WILEY-VCH Verlag GmbH & Co. KGaA, Weinheim), Pressure (Reprinted from the Ref. [179], Copyright © 2017 with permission from WILEY-VCH Verlag GmbH & Co. KGaA, Weinheim), Pulse (Reprinted from the Ref. [180], Copyright © 2018 with permission from Springer Nature), Temperature (Reprinted from the Ref. [181], Copyright © 2014 with permission from Elsevier Ltd.) Humidity (Reprinted from the Ref. [159], Copyright © 2012 Published by Elsevier Ltd.) and Strain (Reprinted from the Ref. [182], Copyright © 2019, American Chemical Society). (b) Resolution and throughput for various printing technologies [183]. Schematic of a (c) R2R (Reprinted from the Ref. [651], Copyright © 2014, Springer Nature) and (d) S2S printing process.

using spin coating, evaporation, inkjet and aerosoljet printing techniques. Inherently organic materials are environmentally friendly as they are biodegradable, exhibit high level of biocompatibility, and are flexible allowing forming into complex shapes. Organic materials with controlled electrical conductivity and ionic transportation make them excellent candidates for transistors and sensing applications [671]. Poly polystyrene sulfonate, PEDOT:PSS exhibits excellent conductivity and chemical stability and also transparent in nature. Furthermore the conductivity of PEDOT:PSS can be improved by secondary doping [672]. PEDOT, polypyrole and poly(aniline) derived materials have demonstrated good biocompatibility and are used in organic electronics [672]. Nevertheless, comprehensive Life Cycle Analysis (LCA) is crucial for every consumer or healthcare electronic device. The LCA should be performed taking into account the manufacturing process, use by the consumer, and after use life (recyclability). As PEs are aimed to be used as wearables and for healthcare applications, ink materials need to be thoroughly investigated for toxicity and alternatives to materials releasing toxicants must be identified.

Screen printing technology and ink properties

Screen printing is a matured technology for PEs as it has been utilized for over 30 years in the solar and electronics industry for printing metal interconnections on Printed Circuit Board (PCB) and solar cells. When compared to other PE process, this technique is faster and more versatile as it brings easiness, affordability, speed and adaptability to the manufacturing method. The minimum thickness of the printed lines (~30 μm) and amount of material used with screen printing also limits the device's flexibility and cost effectiveness of the manufacturing process. In-line metrology plays a critical role in the alignment of the printed lines and within the substrate. The resultant output from this method is possible to reproduce by the repetition of a few processing steps [185–190]. Rotary and flat-bed are the two assemblies of screen printers. Set-up of this technique consisit of substrate, squeegee, screen, and press bed (Fig. 3a). In screen printing, inks are transferred through a stencil screen on to the device substrate, which is made up of a thin sheet of meterials/metals, fine porous mesh of fabric, synthetic fibers or silk [191]. In the non-printing areas, the mesh pores are closed, for example

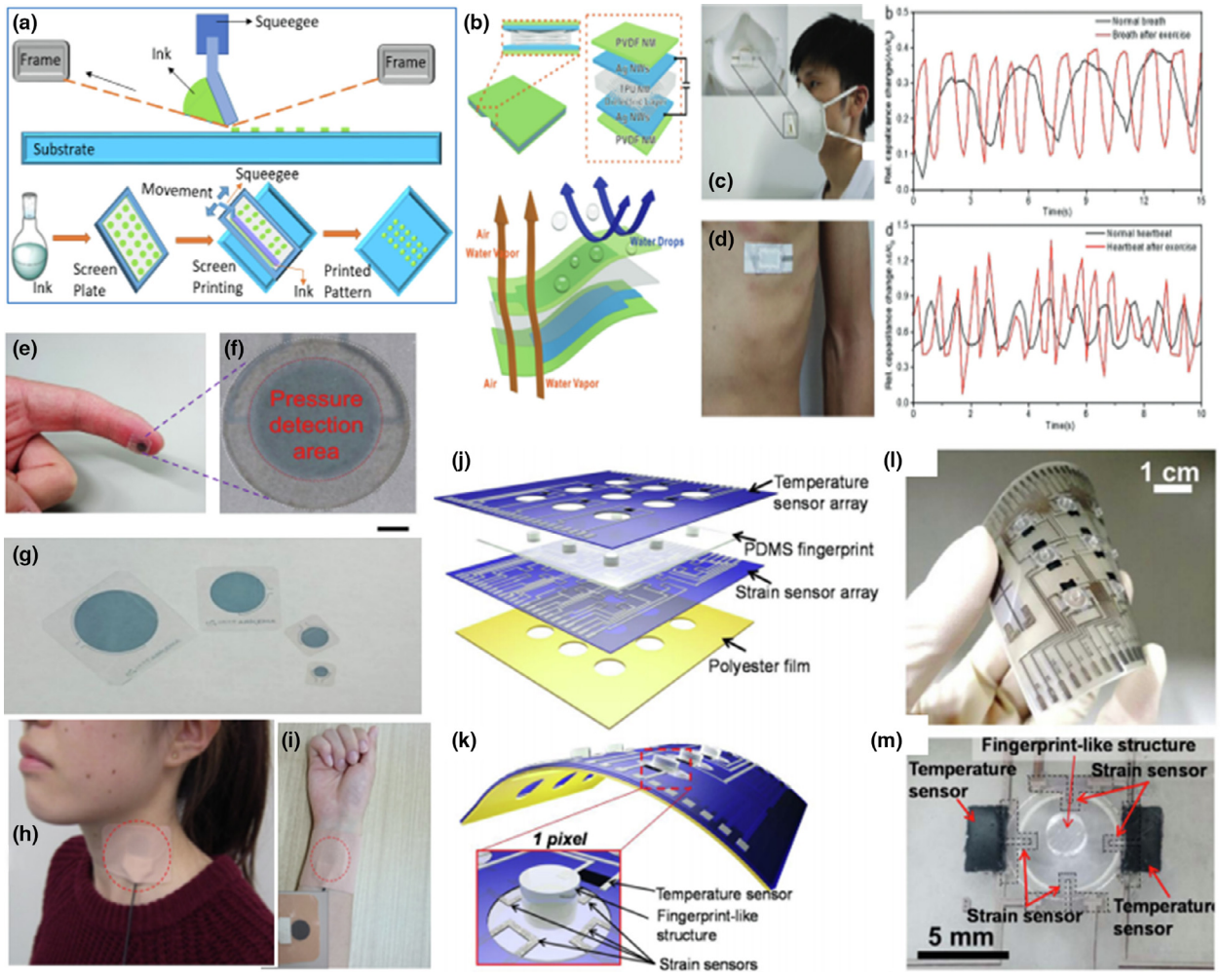

FIGURE 3

Schematic illustration and flexible sensor manufacturing applications of screen printing. (a) Schematic explanation of the screen printing method. (b) Structure and function of the breathable screen printed skin-like capacitive pressure sensor. (c) Screen printed sensor in mask for monitoring respiration and the output of respiration in two different, normal states and exercise condition. (d) Screen printed sensor in the chest for heart rate and signal of the physical force of heart rate under normal state and exercise condition. (b–d Reprinted from the Ref. [206], Copyright © 2017 WILEY-VCH Verlag GmbH & Co. KGaA, Weinheim). (e) Screen printed pressure sensor with high flexibility, laminated on the forefinger and (f) magnified sensor view shown in (e). (g) Photographs of screen printed pressure sensor devices for four diferent sensor sizes of 4, 20, 75, and 130 mm^2. (h) and (i) Images of screen printed pressure sensor attached to the skin using a skin-compatible adhesive patch on the wrist and neck for the realtime monitoring of the pulse wave signal from the blood flow. (e–i Reprinted from the Ref. [180], Copyright © 2018, Springer Nature). (j) and (k) are the schematic of the device which consist a four strain sensors and a temperature sensor and (l) and (m) are the corresponding (l) Screen printed temperature and strain sensor and (m) is an enlarged pixel consisting of four strain sensors and a temperature sensor. (j–m Reprinted from the Ref. [207], Copyright © 2014, American Chemical Society.)

by a photo-polymerized resin, in the printing areas the remaining pores are keep open to permit ink to pass through [192,193]. In the screen printing process, the functional ink spread on the screen mesh at first and a squeegee then force the functional ink through the open pores, in a direction opposite to that of squeegee motion, simultaneously, the substrate that touches the screen start receiving the ink. In this printing method, the mesh acts as both image carrier and ink metering system, thus it determines both the minimum feature size and the deposition thickness. The screen printing process can be utilized to print thick layers of viscous slurries of carbons, conductive metals, insulators or dielectrics. In the rotary screen printing process, it is possible to achieve relatively high speed, however, the rotary set-up screen is very costly and its cleaning is very challenging [194]. Still many flat-bed screen printing methods are containing simple manually functioned components. This will be useful when printing over very thick/very thin substrates that cannot be fed automatically, or if a new image's test run is needed. There are semi-automatic and fully automatic machines available. In a fully automatic machine substrates are fed and taken off by an automatic feed and delivery set ups however, in a semi automatic system, the substrate is taken off and fed in manually, but it uses a mechanized squeegee [195].

The screen printed wearable physiological signal monitoring sensors have been developed. Few examples are given in Fig. 3b–m [180,206,207]. There is a limited range of screen printable inks available and, thus, restricts their performance, purity, and stability in comparison to the use of standard semiconductor materials. Given the lack of standardisation in printable inks, the manufacturing of new devices requires several equipment and

ink adjustments to match the device performance and cost requirements. The volume of ink deposition depends on the factors such as, (i) the thread count of the screen. This is the number of threads per unit distance and thread diameter. (ii) The thread diameter, D. This is the thickness of the screen and the depth of the ink column at each open hole in the mesh. And (iii) the pressure (the angle that in turn explains the area of the squeegee in contact with the screen, and blade speed in respect to the screen during functional ink writing) [192,193,196,197]. According to a model reported by Owczarek and Howland, thickness of the ink (equivalent height of the flow passage) under the squeegee, H_{SC}, can be expressed as [198],

$$H_{SC} = D\left[2 - \frac{\pi}{2}DM\sqrt{1 + (DM)^2}\right] - \Delta H_{SQ} + H_{OA} \quad (1)$$

where D is the screen thread diameter, M is the screen mesh count per inch ($M = 1/m$, and m is the distance between center lines of two parallel wires of a screen, ΔH_{SQ} is the average squeegee penetration height into the screen and H_{OA} is the equivalent open area height. The composition of the ink has a key role in the screen printed patterns. Viscosity [199] and surface tension (γ_{LV}) [200] are the key parameters related to ink composition that affect screen print quality. Viscosities of typical screen printable functional inks are relatively high (~0.5–5 Pa·s, see Fig. 2b) compared to other printing methods. In addition to that, properties of substrate (surface roughness and surface energy (γ_{SV})) [201] determine substrate wettability, also affect print quality. The values of γ_{SV} and γ_{LV} should know to control wetting. If $\gamma_{LV} < \gamma_{SV}$, the surface will wet properly and if $\gamma_{LV} > \gamma_{SV}$, the substrate will show only partial wettability [200]. The thickness of a dry ink deposited on a substrate depends on the pigment and binder in the ink formulation and the solvent as a diluent shows a major part in letting the ink pass through the screen on the substrate and its volatility affects the surface quality of the printed patterns. The printed patterns must be cured (using, either conventional solvent evaporation treatment by heat [202,203] or alternative curing methods include plasma sintering, photonic sintering and laser sintering [204]) for removing solvent to allow patterns functionality after printing. In printed devices, the control of printed patterns conductivities is key to achive high quality functionality and reliability. This printed patterns conductivity depends on the characteristic conductivity of the deposited functional material as well as the printed structures topography.

Phillips et al. have formulated tunable screen printable conductive inks by varying the ratios of graphite and carbon black contents [205]. In their work, they have achived optimal conductivity, 0.029 Ω cm, at a higher total carbon ink loading (29.4% by mass). In this condition, graphite to carbon black ratio is 2.6:1. However, for a 21.7 mass % of carbon loading, this ratio decreased to 1.8:1. Additional increases in total carbon concentration could also further improve conductivity. This highlights techncial considerations which must be taken into account for optimising production and also economic considerations of cost versus functionality.

Inkjet printing and ink properties

Inkjet printing (non-contact technique) [208] has developed as a new wearable flexible sensors/device fabrication method because of its benefits including, low temperature fabrication, various substrates compatibility, additive and digital patterning, fast printing, material waste reduction, and controlled materials deposition [209]. Therefore, this technology has been commonly used in direct printing of electronic parts, such as TFTs (thin film transistors) [196,210], complementary ring oscillators [211], solar cell [212,213], transparent electrodes [214], electroluminescent displays [215], and wearable sensors [216,217]. For printing these devices, nanoparticle and organometallic based inks have been developed using the materials, carbon nanotubes (CNT), Ag, conducting polymers, copper (Cu), and graphene oxide (GO) [218–220]. The solution based material deposition is very easy and inexpensive to produce large area PEs on various flexible (for example, polymers, cotton, synthetic textiles and paper) and rigid (for example, ceramics, metals, glasses and semiconductor) substrates [221–223]. It is possible to use this technique with substrates exhibiting pressure sensitivity or flexible substrates having either non-planar or curved surfaces [224]. An inkjet printer consists of an ink reservoir and print head that has micrometer sized nozzles through which functional inks flow either continuously or drop-on-demand (DoD) to generate images that are designed electronically [225,226]. In this technique, pattern formation consists of generation of droplet, ink spreading on substrate and drying (Fig. 4a). Using this technique, it can accurately deposit materials (micro- and nano-meter sized) into a practical set-up in an additive patterning and maskless approach without any impact [227–233]. This can be controlled by usig a computer.

Drop-on-Demand (DoD) [234–236] and Continuous Inkjet printing (CIJ) are the two modes of operation for inkjet printing technique [240]. CIJ machines deliver droplets stream in which, a droplet is electrically deflected using a set of electronic signal driven discharge electrodes. This printing is used when the quality of the final image is not critical (such as product numbering). DoD systems have a nozzle that supplies ink and a piezo electric crystal (PZT) as actuator. This piezo electric actuator can be excited by an applied voltage, leading to the generation of pressure wave by expanding and contraction, which creates the ink droplet that is then ejected at the end of the ink chamber through the nozzle. In most of the DoD's, a piezoelectric actuator thermally generates the droplets whereas in CIJ systems, the vibrations of piezoelectric actuator lead for passing a continuous stream of electro-conductive fluid through a nozzle, which regulates the fragmentation of the stream into uniform individual drops with an equal spacing [237]. The DoD system allows for a higher control and consistency than that of CIJ systems, due to the reduced complexity of the droplet and flight distance. By far, the majority of reported work using inkjet printing for materials fabrication has reported using piezoelectric DoD systems, however, there has been significant work on thermal DoD as well. Even though CIJ systems have not been used as widely in materials science applications because of the contamination/waste issue, these systems have been successfully used for printing ceramic 3-D objects [238] and conducting Ag tracks [239].

The printing parameters that need to be optimized are ink jetting frequency, inkjetting temperature, diameter of printing nozzles, number of printing nozzles, print height, and inkjetting waveform [240]. In DoD systems, the stable jetting of single ink droplets with each electrical impulse with no satellite droplets formation is a key requirement [227,235,241–243], because, these secondary droplets can lead to ink deposition on untargeted areas and even deviation from the droplet jetting trajectory

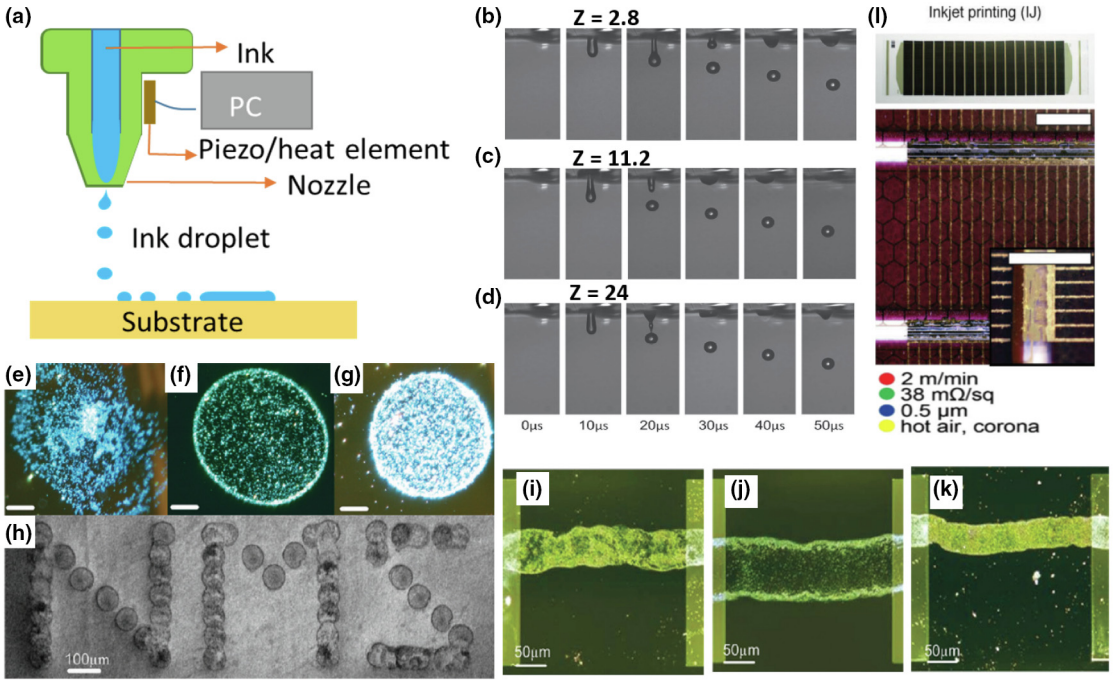

FIGURE 4

Schematic illustration and flexible printed application of inkjet printing technique. (a) Schematic illustration of inkjet printing method. Drop ejection sequences of (b) 80% graphene ink having 20% Ethylene Glycol (EG) having $Z = 2.8$, (c) 20% graphene ink having; 80% EG shows $Z = 11.2$, (d) pristine graphene having $Z = 24$. Dark field optical images of inkjet ink drop on different substrates (e) substrate cleaned using plasma, (f) pristine, and (g) hexamethyldisilazane (HMDS) substrates. Optical micrographs of ink jet printed graphene line is with (i) ~100–110 μm wide, with an average ~70 nm thickness and an irregular distribution of flake, with graphene flakes aggregation, (j) ~130–140 μm wide, shows clusters at the borders and an average ~55 nm thickness and (k) regular and uniform scattering of graphene flakes (width ~85–90 μm and average thickness ~90 nm). (b–k Reprinted from the Ref. [254], Copyright © 2012, American Chemical Society.) (l) Inkjet printed water based Ag ink electrodes (scale bar 5 mm) with printing speed, resistivity, line thickness and sintering factors noted (Reprinted from the Ref. [297], Copyright © 2013 WILEY-VCH Verlag GmbH & Co. KGaA, Weinheim).

[226]. The droplet jetting behavior is determined by the ink fluidic properties, characterized by different dimensionless physical constants, Reynolds number (R) [244], Weber (W) number [245], and Ohnesorge (Oh) [246] number [232,247],

$$R = \frac{\upsilon \rho a}{\eta}, \quad W = \frac{\upsilon^2 \rho a}{\gamma}, \quad \text{and} \quad Oh = \frac{\sqrt{W}}{R} = \frac{\eta}{\sqrt{\gamma \rho a}} = \frac{1}{Z} \tag{2}$$

where a (μm) is the jetting nozzle diameter, υ (m/s) is the average travel velocity of drops, ρ (g cm^{-3}) is the density, η (mPa s) is the fluid's dynamic viscosity and γ (mJ m^{-2}) is the surface tension of the ink. In 1984, it was predicted based on numerical analysis that, the inverse Ohnesorge number $Z > 2$ is essential for a single-droplets ejection without secondary droplets formation in DoD systems [247]. Later, Reis et al., determined using computational fluid dynamics that a printable fluid should have a Z value between 1 and 10 ($10 > Z > 1$) [248]. However, by considering the formability of single droplets, allowable maximum ink jetting frequency and positional accuracy, Daehwan Jang et al., experimentally defined the value, $4 < Z < 14$, in 2009 [249]. Low Z values (<4) indicate the formation of a drop with a long-lived filament and a long time to a single drop generation, may cause secondary drops formation which degrades the positional accuracy and printing resolution. Similarly, the ink with $Z > 14$, indicates the formation of secondary droplets, are also inappropriate for inkjet printing. However, several research groups have been reported this printing with no any secondary drops even for the Z value, $Z > 14$ and $2 < Z < 4$ [235,250–254], *e.g.*, Ethylene Glycol/graphene ink at the concentrations ~80% graphene ink; ~20% Ethylene Glycol and ~20% graphene ink; ~80% Ethylene Glycol, exhibits only individual droplet discharge in these both conditions, as functional inks within the range $1 < Z < 14$, without secondary drops (Fig. 4b–d) [285]. On the contrary to this, pristine graphene ink does not show any satellite droplet formation in DoD printing even if $Z \approx 24$, indicating that other fundamental physical factors not taken into account by Z calculation are at play. In order to optimize ink properties, it is possible to tune Z by varying ρ, η and γ. Typical viscosities of inkjet printable inks are in the range of ~10–30 Cp [208]. The ejected droplets nature on the substrates can be explained by fluid dynamics [255]. The low energy surfaces can give rise to a partial wetting, that results in a finite contact angle θ_c (*i.e.* $\cos\theta_c < 1$) between the liquid and the substrate when the droplet touches on a flat surface [243,249,256,257]. The droplets size limit (s) is,

$$s = a\left[(W + 12)/\left(3(1 - \cos\theta_c) + \left(4W/R^{1/2}\right)\right)\right]^{1/2} \tag{3}$$

A condition used for defining the ink to prevent clogging when it contains dispersed nanoparticles is that their size should be at least 1/50 of the nozzle diameter, that is smaller than the nozzle diameter. This is because if the particle size is larger than the nozzle diameter, it leads to the formation of particle clusters at the edge of the nozzle, may create either agglomeration or drop trajectory deviation that block nozzle eventually [234,236,258]. When a single drop of nanoparticle based ink evaporates, it develops a clear ring pattern on the perimeter of droplet, called coffee-ring effect, which affects the homogeneity of the inkjet printed droplets [234,259,260]. To avoid this condition, it is essential to "freeze" the droplet directly after it forms into the continuous and homogeneous film over the device substrate [227]. The nano particle based inkjet printable ink

deposition behavior mainly depends on the γ_{SV}, ink viscosity and γ_{LV} [234,236]. Another condition that affects homogenous printing and resolution is the distance of nozzle from the substrate [227,241,243]. Since ink-jetting is characterized by noncontact printing, the nozzle must be separated from the substrate during the print process. If the substrate is very close to the nozzle, it may cause satellite droplets to spread off due to the influence of the primary droplet which negatively affects the print pattern. Therefore, accurate substrate to the nozzle distance (typically 1–3 mm), substrate wetting and addition are required [261,262]. The centre to centre distance of droplets (interdrop) is a key parameter for printing lines, because if this distance is large, an individual drop is deposited, so this distance must be smaller than the droplet diameter in order to get continuous lines [263]. However, a very small interdrop distance creates another problem where for example particle aggregation can occur on the substrate, causing non-uniform lines [241,243]. Even though, numerous inkjet printable nanomaterials based conductive inks have been formulated [264–269], they exhibit many restrictions, for example, metallic Cu and Ag nano particles (NPs) [270,271] based functional inks are very costly and they are not even stable in the solvents such as acetone, water, ethanol and IPA. Hence, for the dispersion of these NPs require stabilizing agents in such commonly used solvents [227,272]. Moreover, this class of functional inks often required high temperature sintering post-processing and they get easily oxidized [273]. There are novel technologies such as enhanced NP photo-absorption which allow these inks to be processed more readily [274]. However, as an alternative of these expensive inks, two dimensional (2D) crystals and graphene based inks are developing as favorable cost effective inks [254,275–279]. The first efforts in developing 2D-crystal inks were based on graphene oxide (GO) [272,280–293]. Several research groups have been developed inkjetted reduced graphene oxide (RGO) films for the applications of sensor devices [289,294,295]. Dark field optical images of inkjet ink drop on different substrates are shown in Fig. 4e–h [254]. Fig. 4l shows the inkjet printed Ag back electrodes with process and Ag layer parameters [297].

For wearable sensor applications, conductive patterns with a high resolution can simply be printed using inkjet printer over flexible substrates (Fig. 4i–l) [297]. Inkjet-printed sensors have been advanced for observing strain, temperature, pressure, humidity, and human motion [295,296]. These sensors manufactured using the inkjet printing process depend on the capacitance and piezoresistivity changes. Sensors based on piezoresistivity relay on piezoresistive materials (semiconductor and conductor). By applying mechanical stress their resistance can be changed. The high performance of the inkjet printed wearables depend on many factors including excellent quality of patterns, very good device flexibility/elasticity/stretchability, and excellent durability of devices [223,273].

Gravure printing technique and ink properties

Gravure printing (Fig. 5) is particularly a promising contact printing technique [192,195,298–300]. This method uses direct ink transfer through the physical touching of the structures over the substrate. Cost effective high patterns quality can be produced in this technique. This method consists of a Cu electroplated huge cylinder engraved with micron sized cells, which are filled with ink from an enclosed chamber. Properties of ink and the ratio of microcell width/depth play a key part in this printing process. The depth of microcell varies from 10 to 30 μm and the width of micro cell wall varies from 3 to 5 μm. The minimum printed spot size is 30 μm. This technology offers good image reproduction, variable depth and area printing, and can be used to print on variable rigid/flexible and absorbent/non-absorbent substrates. The TFTs [301], organic photovoltaic devices [302,303], integrated circuits [304] and sensors [305] on flexible/strechable substrates have been manufactured using this R2R gravure printing method.

Many experimental [306–310] and theoretical [311,312] studies have been carried out to determine the optimum conditions to attain high resolution patterning. In this printing technique, ink transfer depends on the ink solvent and viscosity, tracking property, applied pressure and material of the transfer roll. In 2015, Nguyen et al. reported an analytical approach for the ink transfering mechanism in gravure printing which permit an effective process control for printing fine lines [300]. They defined a dimensionless adhesion-force difference (ΔF, which is the difference between the adhesive forces on the substrate (F_{AS}) and cell surface (F_{AC})) for evaluating the functional ink transferring mechanism with respect to γ_{LV}, γ_{SV}, and microcell's surface energy and aspect ratio (AR). The additive forces are $F_{AC} = W_{AC} \cdot L_{AC}$ and $F_{AS} = W_{AS} \cdot L_{AS}$, where W_{AC}, W_{AS}, L_{AC}, and L_{AS} are the contact lengths, L and works of adhesion, W at the ink-cell (AC) and ink-substrate (AS) interfaces. Low γ_{SV} inks, high γ_{LV} substrates, and microcells with high-AR and low surface-energy are appropriate for increasing the ink-transferring ratio during the printing state. In their model, this printing process can be separated in to four different stages: (i) ink phase at the functional ink through, (ii) the doctoring phase where the ink is metered by the doctor blade, (iii) the printing phase where the substrates meets the roller and (iiii) the setting phase where ink is coming out from the cylinder cell to complete printing. The inks moved to the substrate are subjected to F_{AC}, F_{AS} and the cohesive force inside the ink (F_{CO}), (*i.e.*, $F_{AS} > F_{AC} > F_{CO}$). There is no ink transfer occur if $F_{AC} > F_{AS}$ and $F_{CO} > F_{AS}$, over the entire interface. The ink will ideally be transferred if $F_{CO} < F_{AS}$ and $F_{CO} < F_{AC}$. Most of the ink will be transferred to the substrate when $F_{AS} > F_{AC}$, without leaving any voids/pinholes in the printed structure. According to Nguyen *et al.*, the ΔF, which acts as the unit of measure for the success of a R2R gravure printing process in terms of the cell geometry and works of adhesion at the interface as,

$$\Delta F = W_{CELL}\left[W_{AS} - \frac{W_{AC}}{\cos(\tan^{-}[2d_{CELL}/W_{CELL}])}\right] \quad (3)$$

where d_{CELL} and W_{CELL} (Fig. 5a) are the depth and width of a cell, $W_{AS} = \gamma_{ink}(1 + \cos\theta_S)$ and $W_{AC} = \gamma_{ink}(1 + \cos\theta_C)$. Here, γ_{ink}: surface tension of the functional ink, θ_S: contact angle of the ink on the substrate and θ_C: contact angle of the ink on the cell surface. Hence, this printing process largely depends on the γ_{ink} and the ink viscosity which determine F_{CO}. The high cost of gravure rollers dictates that this printing technology can only be used in large scale production of PE devices/components. In this case, the degradation of a doctor blade is used to remove an extra ink from the rotating cylinder, can create printing defects, as well as damage plates and transfer rolls.

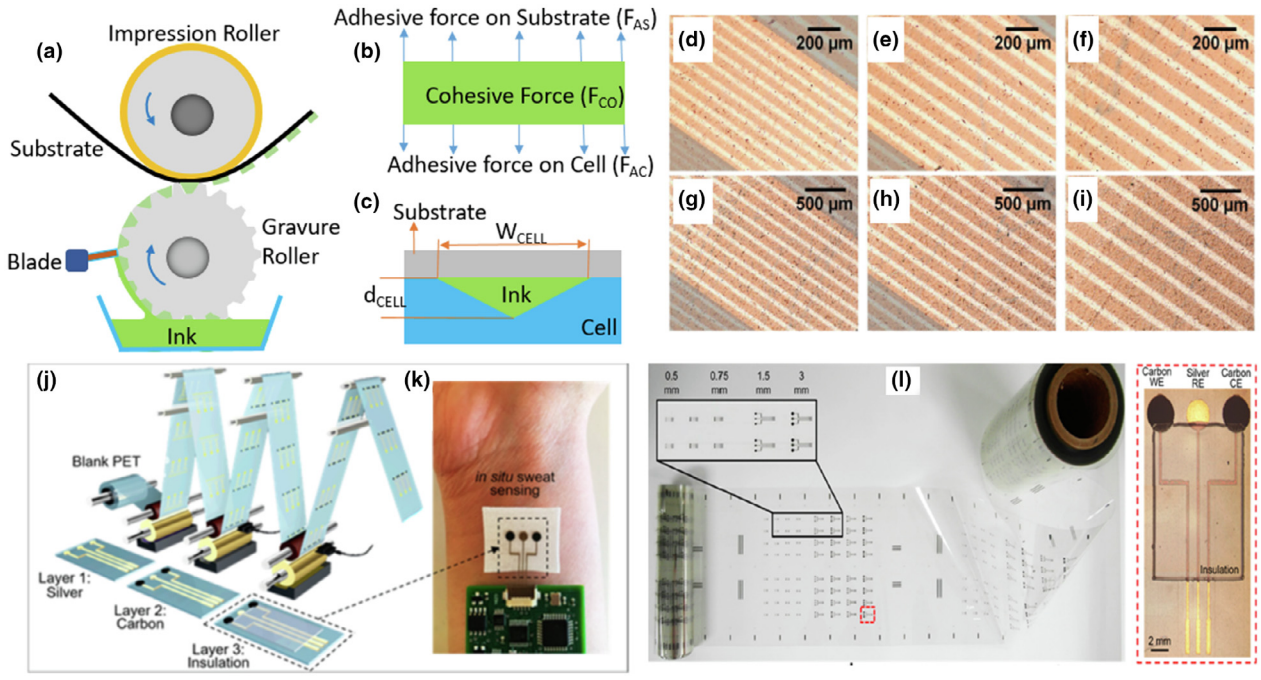

FIGURE 5

Gravure printing principles and gravure printed physiological parameter monitoring sensors. (a) Conventional R2R Gravure printing schematic. (b) and (c) present an overview of gravure printing operation principles. (d)–(i) Optical microscopic images of gravure printed graphene patterns with the trach widths: 15, 20, 25, 30, 35 and 50 µm (d–i Reprinted from the Ref. [314], Copyright © 2014 WILEY-VCH Verlag GmbH & Co. KGaA, Weinheim). (j) R2R gravure printing on PET substrates. (k) Sensor functionalization using gravure printed biocompatible for sweat analysis. (l) Electrodes are gravure printed on a PET flexible substrate of 150 m roll (j–l Reprinted from the Ref. [315], Copyright © 2018, American Chemical Society).

Therefore, these materials must be selected with a great care, especially for large-scale production.

Numerous functional inks have been developed for this printing technology [313]. In 2014, Secor et al., formulated a high-concentration stable graphene functional ink in an environmentally and chemically benign solvent and then gravure printed high-resolution large-area patterns on flexible substrates (Fig. 5d–i) [314]. In that work, electrically conducting lines (~10,000 S/m) having ~30 µm resolution have been fabricated on large areas with an excellent uniformity and reliability.

Recently, transparent electrodes and interconnects have been gravure printed using one dimensional (1D) nanomaterials based inks (*e.g.* metal nanowires ([316,377,378]) and CNT [318,319]) on flexible substrates [315]. In 2018, Huang and Zhu developed gravure printable water-based Ag nano wire (NW) ink for flexible substrate [320]. They report that by tuning the properties of ink, processing conditions and post-processing treatment, a highly conductive (~5.34×104 S cm^{-1}) and high resolution (as fine as 50 µm) Ag NW patterns can be gravure printed over large-areas. Under different bending cycles, these Ag NW lines on the PET substrate displays exceptional robustness and flexibility.

Flexographic printing technique and ink properties

Flexographic printing is a continuous contact method that uses a flexible image carrier/plate made from rubber or polymer (Fig. 6) [183,321]. This process is used for high speed runs of PEs. In this printing method, the ink is moved over the substrate that positioned on an engraved anilox roller (which is an ink metering device) and then, after the removal of the excess ink using doctor blade from non-engraved surface of the anilox, the relief areas of image pass to the printing-plate, called flexoplate. Using an anilox roller, the developed structure on the flexoplate is covered by a homogeneous layer of functional ink. This roller surface is made up of number of small wells or cells for carrying a specific amound of functional ink. The cell depth in the anilox roller is constant, that results a constant thickness of inks being transferred to the plate roller. Here, the support thin substrate, called as the web, should be soft and flexible for wrapping over the anilox roller. The patterns are generated when the ink coming out from the impression roller is transferred to the substrate. Minimum printed spot size noted as 20 µm [322]. This method requires only a slight contact pressure to allow reliable transferring of ink from the printing plate to the substrate. Flexible printing plates enable quality imprints even with a low and gentle contact pressure within the printing plate and substrate [321]. Major driving forces behind the constant improvement of the flexographic print quality are the technologies related with the creation of the printing plate, ink formulation and the anilox delivery systems. This technique is suitable for substrates such as very thin, flexible, and solid materials, virtually all papers, thick cardboard, rough-surfaced packaging materials and fabrics [323]. Like gravure, the flexographic printing process starts with inking and doctoring of the anilox roller, however, unlike gravure, these anilox cells are not the key image generating area and are responsible for metering the volume of functional ink for ensuring the development of continuous and homogeneous patterns [324]. Many anilox cell structures such as, pyramid cells, tri-helical, quandrangular *etc.* are used in this printing method.

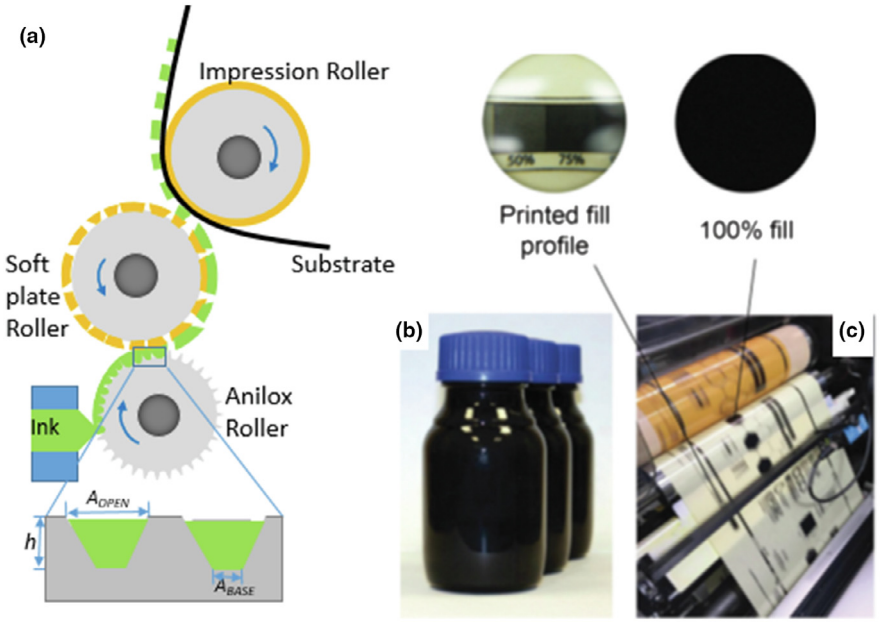

FIGURE 6

Flexographic printing principles, flexograhic printable functional ink. (a) Flexographic printing schematic and its principles. (b) Flexographaic printing ink trialed on (c). Inset shows zoomed in pictures of the printed fill profiles (b–c Reprinted from the Ref. [324], Copyright © 2018, Royal Society of Chemistry).

The amount of ink that a single anilox cell (V_{CELL}) can hold in a pyramid cell structure is calculated as,

$$V_{CELL} = \frac{h}{3}\left(A_{OPEN} + A_{BASE} + \sqrt{A_{OPEN}A_{BASE}}\right) \quad (4)$$

where A_{OPEN} is the cell opening area, A_{BASE} is the area of cell base and h is the height of the anilox cell (see Fig. 6a). This equation differs between cell structures.

Both these, gravure and flexo, technologies relay on large metal rolls, gravure roller and anilox roller (engraved cylinder that transfers the ink onto the printing form), to control ink deposition on the substrates [325]. Gravure is a 'direct' printing method in which functional ink brings from the ink through to over the substrate directly through the roller which not only meters the wet ink application weight but also acts as the print image carrier. However, flexographic printing, is an 'indirect' printing process upon which the control of the wet ink application weight is implemented via the anilox roller, transferring the metered ink from the anilox to an image plate, before the ink deposition onto the substrate. Both of these printing techniques are strong practical candidates for high-speed, cost effective fabrication of 2D material printable applications due to their high throughput. In these techniques, successful printing demands the homogenious and controlled ink transferring mechanisms onto the substrates [326,327]. The fators that affect this critical stage is solvent of inks, pressure and materials of transfer roll [326,327]. These printing methods require very high volatile solvents because, these processes run at very high speed and the inks dry mostly by evaporation [328].

R2R is considered to be a leading technology that need to be matured to produce inexpensive flexible PEs in the near future since it enables mass scale production by high speed web handling. Screen and inkjet printing techniques are commercially used for manufacturing of PEs. Gravure and flexographic techniques are still at low TRLs and require further research and development activities to commercialise. Nevertheless, a general comparison of these printing techniques and their ink formulation specifications are given in Table 1.

3D printing

Multi-material Additive Manufacturing (AM) enables fabrication of complex electronic components with customized designs such as radiofrequency (RF) transmitters and receivers, filters, and circuit tracks with reduced size, lightweight, and lower power consumption. Most AM techniques use single material to print complicated 3D parts. A number of multi-material AM systems are commercially available that can print conductive functional tracks and polymer housing in single run. These systems have enabled a number of research groups to print electronic devices (RF, filters, temperature detectors), volumetric electrical circuits, and electrical interconnects [334–338]. Inkjet printing, fused deposition modeling, stereolithography, and 3D material jetting are major 3D printing techniques used for electronic components. Mirotznik et al. demonstrated additive manufacturing of transmission lines, antennas, and connectors for radio frequency devices using nScrypt 3Dn-300. Lower conductivity of AM produced functional tracks is still challenging and use of hybrid techniques allow improvement of conductivity in printed tracks. UV irradiation was used to sinter the 3D printed arbitrary structures to fabricate polymer bonded permanent magnets [339]. In other multi-material 3D printing work, a non-grounded coplanar waveguide (CPW) configuration was printed and immersed in electroplating solution to metallized the conductive structures [340]. Scattering parameters were improved after electroplating of the printed waveguide. The surface roughness of 3D printed components is still high compared to other fabrication techniques.

TABLE 1

Comparison of printing techniques and their ink formulation requirements [192,195,298–300,329–333].

	Inkjet	Screen	Gravure	Flexographic
Printing form	Digital	Stencil/R2R	R2R	R2R
Approach of printing	Non-contact	Contact	Contact	Contact
Printing speed (m/min)	15–500	10–15	100–1000	100–500
Minimum line width (μm)	30–50	30–50	10–50	45–100
Solution surface tension (mN/m)	15–25	38–47	41–44	13.9–23
Resolution of printing (μm)	15–100	30–100	50–200	30–80
Speed (m/min)	0.02–5	0.6–100	8–100	5–180
Substrate	Flexible	Flexible	Flexible	Flexible
Process mode (step)	Single	Multiple	Multiple	Multiple
Mask requirement	No	Yes	No	No
Material wastage	No	Yes	Yes	Yes
Ink composition (wt%)				
Pigment	5–10	12–20	12–17	12–17
Binder	5–20	45–65	20–35	40–45
Solvent	65–95	20–30	60–65	25–45
Additive	1–5	1–5	1–2	1–5

Considering the 3D printing of electronic components, innovations in consumer and healthcare electronics are required that enable the production of slim, lightweight, and smart devices connected with each other. The viscosity provided from the ink is a limitation in selection of material-process arrangement for PEs. The aerosol Jet printing technique provides a complete solution that enables the fabrication of 3D printed electronics without use of masks or stencils. Inkjet printing cannot be used for multi-layer and multi-material printing, where functional devices in multilayer format are stacked over each other. In such cases, each electronic component (*e.g.* photodetector, transistors, and LEDs) has to be printed with a different material (*e.g.* conductive or semi-conductive materials, resistive materials, and dielectric and encapsulation materials) having a different viscosity [673]. Aerosol jet printing enables printing of materials with different viscosities. This technique is rather simple in which an inert gas is used to atomise the ink material. The type of atomiser depends upon the viscosity of the ink material. For lower the viscosity range (1–5 centipoise) ultrasound atomisers are used. However, for ink materials where the solvent has high viscosity (up to 1000 centipoise) pneumatic atomisers are used. As the inert gas flows over the ink surface, a mist is generated with droplets of the ink material. Big droplets (over 5 μm) settle while the small droplets (less than 5 μm) are collected and driven towards deposition head. The aerosol density is increased in the next step by removing the extra gas using a virtual impactor. The concentrated aerosol stream is compressed and focused using a sheath gas (dinitrogen) as it passes through the nozzle of the deposition head resulting in printed fine structures that are of less than 10-μm resolution. This technique allows conformal printing on flexible substrates with complex geometries as no physical contact is required between the deposition head and the substrate. The distance between the nozzle and substrate can be varied between 1 and 5 mm. This flexibility in the distance enables aerosol printing on non-planar surfaces. Freeform deposition of aerosol is made possible by using computerised precision motion and mechanical shutter system control. A wide range of materials can be printed using aerosol jet printing. Conductive nanoparticle colloids (*e.g.* Au, Ag, Cu, Zn, and Graphene etc.) have been used to print interconnects and conductive tracks [674–677]. Li-ion based battery cathodes fabricated with aerosol jet printers have shown improved discharge capacities [678,679]. Achieving high volumetric efficiency is the biggest advantage of 3D printing while multi-material printing using aerosol jet printing allows the printing of electronic devices with high volumetric efficiency [679,680].

Printed electronics inks and substrates

In electronic device manufacturing, PE is becoming increasingly a method that promises to enable a large number of applications through integrating functional inks with conventional printing technologies. Inorganic and organic materials are used for ink formulation [341]. Normally, inorganic materials ink consist of metallic NPs, for example, Cu, Au, Ag, aluminum (Al). Organic inks contains materials including polymers, carbon black, RGO and graphene *i.e.,* dielectrics, semiconductors and conductors. The conductive polymer based ink has been used in sensors, resistors, electromagnetic shields, inductors, batteries, capacitors, *etc.*, whereas organic semiconductor based ink is employed in active devices as active layers. The PE ink is composed of a particular material and many other additives including surface tension and rheology modifiers, agents, defoamers and binder that dispersed or dissolved in an organic or aqueous solvent [192,298,329]. In the PE ink, the functional materials are incorporated into the ink systems as active agents (*e.g.*, various conducting, semiconducting and dielectric materials) [342,343]. These inks are then pattern onto a substrate for functional device fabrication. The print pattern homogenity and its properties are heavily dependant on the ink formulation. The compatibility of sovents to the functional materials and the selection of an appropriate formulation mechanism for the functional material carrier are important factors for developing homogeneous functional inks. The functional ink formulation mechanism mainly involves varnish (liquid carrier) developement, pigment (functional material) dispersion and composition turning for adjusting the physical properties of inks. The physical properties of

the varnish, which is usually prepared by dissolving additives and binders in the solvents (is the diluent to the functional materials, additives and binders), define the wetting properties of the functional materials and thereby govern the properties of the functional ink [192,329]. Varnishes are categorized into water based and organic solvent based. Highly volatile ethyl acetate, IPA and *n*-propyl acetate are the solvents usually used for the high speed gravure and flexographic printing process as these require rapid drying of the ink. However, slighly low volatile solvent such as butoxyethanol and aromatic distillates, having moderate evaporation rates, are used for the screen printing process for avoiding screen mesh clogging associated with the fast drying of the ink. As water is an environmentally friendly solvent, there is a high demand for the developement of water based functional ink formulations. The varnishes that carry functional materials onto the flexible substrate solidify after the complete evaporation of the solvent. For blending the functional material/pigment into the varnish, various dispersion technologies such as, ball milling, agitation, high speed mixing, and three-roll milling are used [298,329]. For low viscous inks, that are used for the inkjet printing method, suitable blending processes are ball milling and agitation. High speed mixing processes are used for the medium viscous inks which are suitable for the flexographic and gravure printing techniques. For high viscosity ink systems commonly used for screen printing technology, the suitable blending method is three-roll milling [298,329].

Recently, there is much attention directed toward investigating the solution-processed 2D materials as functional agents as a way to exploit their unique material properties [344,345]. The 2D material printed application was first reported in 2012 by Torrisi *et al.*, when graphene was ink jetted to produce field effect transistors [254]. Since then, rapid advancements have been witnessed in 2D materials ink formulation and production of devices. Examples of 2D material agents are transition metal dichalcogenides (TMDs), black phosphorus (BP) and hexagonal boron nitride (h-BN) *etc.* [276,346–350]. However, these first generation of 2D material based inks were not optimized for the advanced printing technologies, *e.g.*, inkjet, screen, flexo and gravure printing [314,351–356]. Therefore, this new class of inks are just emerging. The main applications of printable 2D materials include optoelectronics, conductive inks, photonics (*e.g.* nonlinear optical devices), sensors, and energy storage (*e.g.* super capacitors and batteries) [276,314,346–355,357–362]. Controlled additive patterning of the 2D materials has also enabled the manufacturing of fully-printed heterostructures (*i.e.* stacks of multiple 2D materials) [346–348]. The other component, binders, are typically polymers [348,357], that allow to bind the material particles to each other and onto the substrates. These binders dry up and solidify very easily by evaporation of solvents. However, in some cases, this may need curing, for *e.g.* sintering/annealing or ultraviolet light radiation exposure in order to crosslink. Examples of binders for flexible printed devices are acryclic [363], silicone [364,365], styrene [366], fluoroelastomers [367], or urethane [368]. Another key component of the functional ink is solvents. These are providing excellent binder solubility and offer satisfactory ink viscosity, homogeneity and surface tension. Solvents are keeping ink fluidity by mixing/diluting other ink components such as agents, binders and additives such that the ink can be applied to the printing press until it is transferred to the substrate. Wetting properties of the substrates and agents can be improved by using additives (*e.g.,* surfactants). For specific applications, inks properties have been tailored by using the surfactants [369,460], adhesion improvers [365,370], humectants [371], penetration promoters [372], and stabilizers [373].

More recently, one dimensional (1D) materials (nanotubes, nanowires, and nanoribbons) got attracted due to their significant properties (mechanical, thermal and electrical) from the formed bulk materials. Among the 1D materials, CNT based inks are very promising and highly suitable for flexible electronic applications. Theoretically, it has been shown that maximal strain that the CNTs can reach to is 15%, indicating the high flexibility of CNTs [374] which has been identified also by experimental results [375,376]. Compared to the metallic inks, the conductivity of CNTs is poor, which results in their limited applications and performance. Recently, metallic NWs based inks aroused immense interest of researchers. Lee et al. developed a highly stretchable and highly conducting metal electrode that was fabricated using long Ag NW based ink [377]. Even in the stretched state, the patterns based on this Ag NW ink shows high performance. A significant feature of nanomaterials for the sensing platform application is thier physical properties tunability. For the development of wearable sensors, numerous 1D and 2D materials based inks that consist of a wide range of materials including, nanofibers [32,71,206], nanowires [31,39,44,75,279,317], nanotubes [40,267,318,379–382], graphene [276,285,357,383,384], metal-based nanoparticles [140,385–389], and quantum dots [390,391] have been formulated. Mainly, those printable inks are formulated for inkjet [357] screen [392] gravure and flexographic [314] printing technologies.

The significant physical properties that affect deposition of the ink on the substrates are: surface tension, viscosity, density and drying rate [221]. For a particular printing technique, ink viscosity (which is a rheological description of a fluid with respect to the shear stress, the shear rate and the shear time [393–395]) is a key consideration and critical parameter related to printing ink selection. Generally, fluids are categorized into non-Newtonian and Newtonian. If the viscosity of inks remains constant, these are Newtonian, whereas non-Newtonian fluid viscosity may change depending on applied shear stress, therefore inks can spread easily when pressure is applied [396]. Due to this, Non-Newtonian inks are favoured for printing technologies. Different printing technologies need specific properties of inks for achiving a particular resolution and performances. Viscous inks are required for screen printing whilst highly fluent, low viscosity fluids are desired for inkjet printing. The preferred PE inks must exhibit good printability. These inks should satisfy the needs, such as, the preparation process of the inks should be simple and have a high yield.

Also, the surface tension and viscosity of these inks must be located within a suitable range to make them compatible with a number of printing technologies. In addition to that, without any precipitation these inks must be stable for months at lower room temperature and the materials should be sustainable [371].

Dielectric based inks

Insulator PE inks should have excellent insulation capabilities, which is also often used as an encapsulation to prevent metallic ink oxidation in PE fabrication. The direlectric inks and substrates for the PE applications have been developed from organic/inorganic hybrid dielectrics, inorganic materials, and polymers [397,647]. In these, metal oxide inorganic dielectric materials having a higher value of dielectric constants recevied much attraction. Dielectric inorganic materials (for example, alumina (Al_2O_3) and silica (SiO_2)) require high temperature processing in order to produce bonding of the dielectric high-density films. A fully printed metal–insulator–metal capacitor on a flexible substrate has been developed using HfO_2 (hafnium oxide) and Silver metal *i.e.*, Ag/HfO_2/Ag, by inkjet printing method [398]. The dielectric strength of HfO_2 material is high. This developed capacitor by Vescio et al. exhibits excellent reliability and homogeneity. When considering organic dielectric materials, their processing temperatures are very low and they exhibit good flexibility and higher values of dielectric constant. Due to these propertires, organic material is desirable for PE applications. The polymer insulators normally used in electronic applications are polystyrene (PS), PI, poly(4-vinylphenol) (PVP), PET, polypropylene (PP), poly(methyl methacrylate) (PMMA) and polyvinyl alcohol (PVA). In 2014, Withers et al., have developed hexagonal h-BN based dielectric ink for inkjet printing of gate dielectric for devices based on heterostuctures (Fig. 7a and b) [421]. h-BN is a hexagonal crystalline form of boron nitride with a layered structure and its inks has been developed in water using the salt of 1-pyrenesulfonic acid sodium [399,400]. This material is called white graphite. It shows good thermal and electrical properties. Since the material has wide band gap (~6 eV), this in combination with the dangling bonds absence and smooth atomic surfaces, h-BN makes an ideal candidate as dielectric substrate for the 2D material based inks in hetero structure device fabrications [401–403]. The h-BN ink shows an exceptional chemical, mechanical, thermal and optical properties and hence, this will be an alternate dielectric material in future for the development of next generation nanodevices [404–409]. In 2017, Carey et al., have formulated dielectric h-BN ink curable at room temperature, having Z ~19.4 (for h-BN) for DoD system (Fig. 7c and d) [361]. The rheological parameters (η, γ and ρ, see Section "Inkjet printing and ink properties") of this dielectric ink are, $\eta_{h\text{-}BN}$ ~1.7 mPa s, $\gamma_{h\text{-}BN}$ ~72 mN m^{-1}, $\rho_{h\text{-}BN}$ ~1.01 g cm^{-3}. For the ink formulation, they have used deionized water as solvent and carboxymethylcellulose sodium salt (Na-CMC) as additive. The lateral dimension of the h-BN flakes varied from 516 nm to 5 μm which was in agreement with the general guidelines of inkjet printing where the average particle size should be <1/50th of the nozzle diameter to avoid nozzle clogging [254].

Semiconductor inks

In electronic components, semiconductors show prominent roles. For producing semiconductor thin films, most of the fabrication techniques use a sputtering process. Even though, the solution-processing approaches have been employed to fabricate semiconductor devices, these suffer from poor device performance. The ink based on organic semiconductors has greater flexibility and processability. After deposition of solution, these only require evaporation of solvent. These materials are considered as appropriate for wearable flexible PEs due to its ability to process at lower temperature with different flexible substrates make. For inkjet PEs, the semiconductor inks are possible to prepare either from organic polymeric semiconductors including P3HT (poly(3-hexylthiophene)) [410,411] and PQT-12 (poly[5,5′-bis(3-dodecyl-2-thienyl)-2,2′-bithiophene]) [285,412–415] or soluble organic semiconductors of small molecule, for example, pentacene derivatives (6,13-bis(triisopropylsilylethynyl) (TIPS-pentacene)) [416,417] or benzothiophene derivatives (BTBT) [418].

The inorganic semiconductors usually have higher durability, superior device performance and stability. Therefore, recently, interest in inorganic semiconducting nanomaterials are increased because of its huge potential applications in large area and inexpensive PE devices. Oxides of transition metals (*e.g.*, ZnO TiO_2, CuO, MoS_2, SnO_2 and In_2O_3, and its derivatives), perovskite, kesterite and silicon are the typical inorganic semiconductor materials used in PE components/device fabrication [419–422]. For example, Gebauer et al., have recently produced

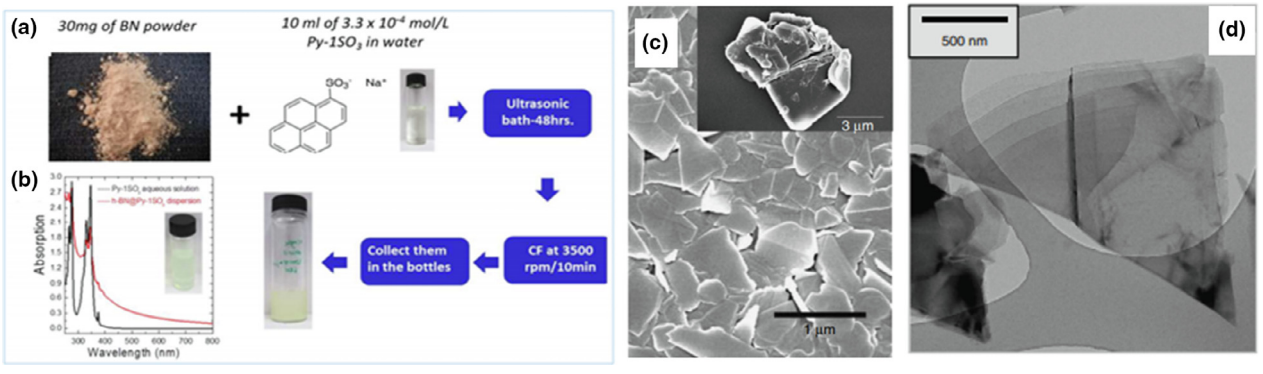

FIGURE 7

Dielectric ink formulation and its characterization. (a) Schematic illustration of the h-BN ink formulation in Py-1SO_3 aqueous solution and (b) optical absorption spectra of Py-1SO_3 and Py-1SO_3_h-BN solutions. (a and b Reprinted from the Ref. [346], Copyright © 2014, American Chemical Society). (c) Scanning electron microscopy images of h-BN flakes ~516 nm and (d) transmission electron microscopy micrographs of h-BN flakes. (c and d Reprinted from the Ref. [361], Copyright © 2017, Springer Nature.)

different metal oxide nanoparticles (ZnO, TiO_2, CuO, SnO_2 and In_2O_3) based inks [423]. Nanoparticles of these metal oxides are synthesized by chemical vapor synthesis (CVS), yielding small particles with high crystallinity and phase purity. These metal oxide inks exhibit long-term stabilities without particle sedimentation over a period of several months with rheological and interfacial properties suitable for inkjet printing on different substrate materials like silicon and flexible polymeric substrates.

Schneider et al. studied a series of zinc complexes with oximate ligands for their suitability as precursors for inkjet printing ZnO, and presented that ZnO microstructures could be used in PE device manufacturing [424]. As shown in Fig. 8, Cui et al., have developed ZnO NPs based inks and screen printed them as patterns, ZnO NW array via a hydrothermal method, on PET substrate and Si wafers [425]. This site-selective growth mechanism was used to grow the patterned ZnO NW array from the ZnO NPs. These NW arrays with uniform morphology exhibits hydrophilic and lipophilic properties and the patterns of these could be easily controlled by the screen printing plate. Recently, several 2D semiconductor materials inks are used and inkjet printed over various substrates for the fabrication of PE devices [426–428]. Indeed, the liquid exfoliation of layered materials is often used to develop inkjet printable inks to manufacture PE devices [345,429,430]. For example, Li et al. reported an efficient and a reliable technique for inkjet printing of multilayer MoS_2 nano sheets (>6 layers, 5–7 nm thick) [431]. This technique enables the integration of inkjet printed MoS_2 patterns with other components, and therefore allows the construction of various functional PE devices. Even though the inorganic semiconducting inks are environmentally stable and providing higher electric performances, these exhibit disadvantages including post processing treatement at higher temperatures and insufficient dispersions. These properties are not compatible to the flexible substrates which are used for wearable electronics applications [432].

Conductive ink

Metal nanoparticles, typically synthesized in solution [433–436], are important in the fabrication of advanced components/devices. These are offering numerous opportunities for the development of miniaturized PEs [437], and sensors [438]. For conductive PE inks, the printed patterns should possess high room temperature conductivity and upon sintering, obtain bulk conductivity at a lower temperature (<150 °C). Conventional materials based on metals (*e.g.,* Ag, Au, Cu nanowires/nanoparticles/flakes [26,439,440]) and carbon (*e.g.,* CNT [441–443] and graphene [444-447]) are generally considered for developing conductive printable inks/pastes for printing components/devices [448–452].

Organic inks: Carbon based conductive materials have been considered (especially developed from the carbon black and graphite), in the production of coatings and inks in the PE applications [453–459]. Carbon based nanomaterials exhibits greater sensitivity and an excellent mechanical and electrical properties [24,353,430,460,461]. Since the development of graphene (basic building structure of graphite), this has been used in numerous applications such as sensors [462–464], energy storage devices, [465], fuel cells, [466], high strength materials, [467], biomedical sector of therapy [468–470] diagnosis [471–475] and drug delivery [476–480] due to its significant properties larger surface area [481], high electrical conductivity [482], higher strength, [483], high thermal conductivity [484], good elasticity [485], chemical inertness [486] and gas impermeability [487]. Over the past decades, graphene oxide (GO) has been extensively studied [488–493], and several research groups have reported on development of GO based inks [272,281,294]. GO is produced by graphite

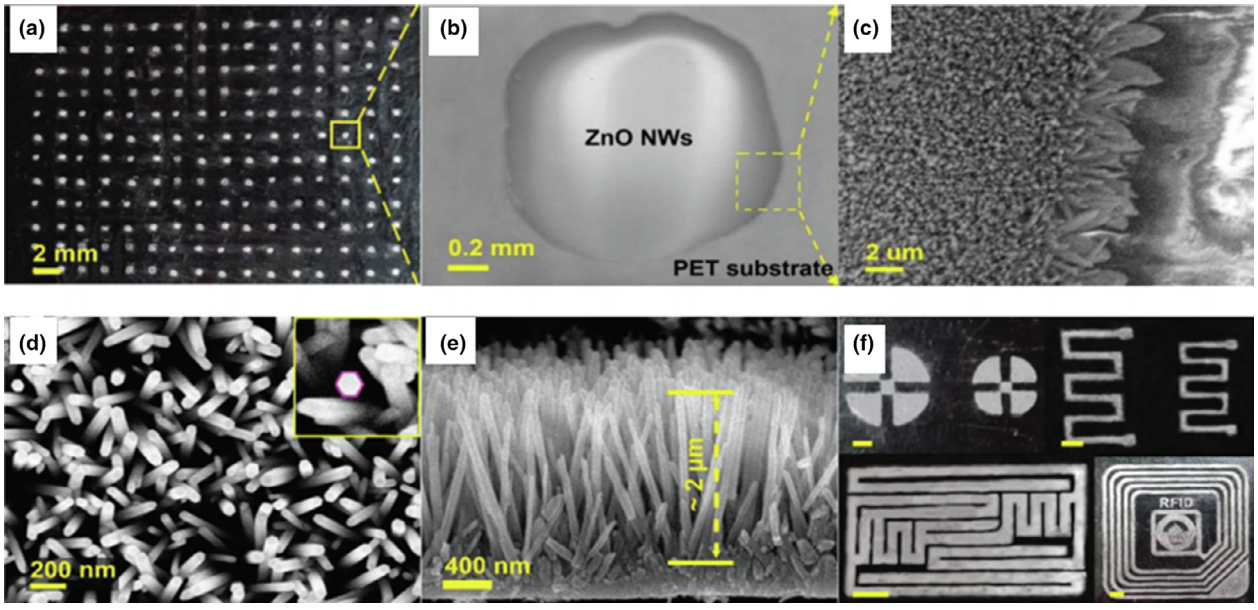

FIGURE 8

Zincoxide nanowires with its characterization and application. Images (a)–(d) are selectively grown ZnO NW array on PET by screen printing of ZnO NPs based ink and a hydrothermal process; (e) the cross sectional SEM pictures of site-selective growth of ZnO NW arrays; (f) photograph of different ZnO NW array patterns. (Reprinted from the Ref. [425], Copyright © 2016, Royal Society of Chemistry.)

oxidation with oxidants or acids [494,495], which disturbs the network of sp^2 hybridization. This disruption creates the group of either epoxides or hydroxyls, with carbonyl or carboxylic groups attachement to the edge [496,497], making GO readily dispersible in water [493,498] and other solvents [499]. Borini et al., have developed highly flexible and transparent temperature and humidity sensors suitable for the large volume fabrication using GO ink (Fig. 9) [500]. The sensor was shown to have a very fast response time in detecting moisture in a user's breath (~30 ms response and recovery times). Selected PE organic inks for the application of physiological signal sensing devices are given in Table 2.

Inorganic metallic inks: Among the advanced materials used for sensor fabrication, nanowires or nanofibers of inorganic materials are widely studying due to the properties such as high sensitivity and simple assembly [154,503–506]. In one of the early studies, Dearden etal. synthesized a lower temperature organic Ag ink for the application in a drop on-demand inkjet printer. Very recently, conducting inks that dry at room temperature and form an instantly conductive layer, without the need of time-consuming sintering process have been developed [507]. These inks are, therefore, suitable to be cheaply and easily deposited on a flexible substrate. Selected PE inorganic metallic inks for the application of flexible physiological signal sensing devices are shown in Table 3.

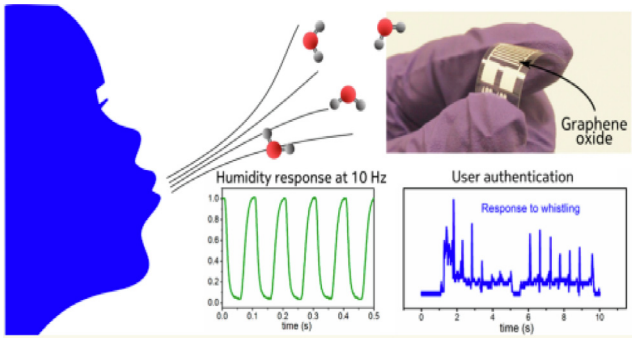

FIGURE 9

Humidity sensor based on graphene oxide. Wearable and flexible sensors fabricated using conductive organic ink. Graphene oxide (GO) based flexible humidity and temperature sensor capable of measuring breath humidity and distinguishing human behaviors such as whistling (Reprinted from the Ref. [500], Copyright © 2013, American Chemical Society).

Composite ink

The conductivity and stretchability of printable composites need to be improved for the practical PE application when compared to the highly conductive metallic ink. The theoretical prediction of composite conductivity expressed as,

$$\sigma = \sigma_0 (V_f - V_c)^s \quad (5)$$

where σ: electrical conductivity of the composite, σ_o: conductivity of the conductive filler, V_f: volumetric fraction of the filler, s: fitting exponent and V_c: volumetric fraction at the percolation threshold. Printable composite ink has been synthesized using SWNTs (ultra-long single walled carbon nanotubes) and fluorinated copolymer in ionic liquid [516]. This ink exhibits 57 S cm^{-1} conductivity at 38% of tensile strain. Chun et al., reported printable hybrid composites with a high conductivity and stretchability. This ink contains flakes of micrometer-sized Ag and multi walled CNTs in combination with self-assembled Ag NPs [451]. This printed hybrid Ag–CNT composites exhibit conductivities 5710 S cm^{-1} without strain and 20 S cm^{-1} with 140% of strain [451]. Selected PE composite inks for the application of physiological signal sensing devices are displayed in Table 4.

Electro conductive adhesives: Reliable and highly conductive electrical interconnections are still challenging in PEs. Different epoxy-based metallic pastes were used previously but are prone to cracks and detachment on stretching of flexible substrates. Over the last years there has been extensive research on Electro-Conductive Adhesives (ECAs) materials and process improvement leading to innovative solutions which provide increased functionality due to higher conductivity. By avoiding use of lead and tin, these materials offer more environmentally friendly solutions to join different electronic components.

Reactive ink

Reactive ink (based on colloidal NP) is emerging as a strong substitute for NP based ink in PE application, especially in the fabrication of conductive metal tracks or electrodes. This class of inks called as metal organic decomposition (MOD) ink [239,521–524]. These inks are aqueous solutions that reduces the clogging. In this class of inks, colloidal stabilizers are not required, hence, very suitable for inkjet printing. The concept of inkjet printing using reactive inks (or called reactive inkjet printing) is using inkjet printer to combine droplets of two reactants. This technique consists of two process, (i) printing of metal precursor and (ii) then depositing a reducing reactant at the same place to attain the elemental metal directly on the substrate (Fig. 10) [525]. This method has the advantages of being fast, inexpensive, and appropriate for productions in large-scale, and provides an

TABLE 2

Selected examples of printable organic inks and their physiological parameter monitoring wearable sensor applications.

Ref	Functional organic inks	Solvent	Binders, cross linker	Substrate	Curing temp (°C)	Ink property	Sensing application
Inkjet printing							
[501]	Graphene	Diethylene/ ethanol	PEDOT: PSS	PU	70	Conductive	Temperature
[89]	CNT	Water	PEDOT:PSS	Kapton	100, 10 min	Conductive	Temperature
Screen printing							
[502]	CNT	Water	UV light	Textile	30	Conductive	Strain
[502]	Carbon Black	Ethanol	Poly acrylic acid-A and Poly acrylic acid-B	Paper		Conductive	Strain

TABLE 3

Selected examples of printable inorganic metallic inks and their physiological parameter monitoring wearable sensor applications.

Ref	Metallic inks	Solvent	Binders/crosslinker	Substrate	Curing temp (°C)	Ink property	Sensing application
Inkjet printing							
[508]	AgNP	1,2-Dichlorobenzene	–	KAPTON	150	Conductive	Strain
[509]	Ag	–	–	PI	130, 10 min	Conductive	Temperature
[510]	Ag	–		Paper		Conductive	Temperature
[511]	AgNP	Hexyl acetate	Pressure of 170 kPa (5 min at room temp.)	Kapton foil	60, overnight	Conductive	Temperature & Humidity
[512]	AgNP	–	–	Paper	150, 30 min	Conductive	Temperature and Humidity
[512]	AgNP		UV light	PET	150, 3 h	Conductive	Temperature and Humidity
Screen printing							
[513]	Ag paste	–	–	Textile	130, 10 min	Conductive	Strain
	Polymer	–	–	Textile		Dielectric	
[514]	Ag	Water		Textile	80, 25 min	Conductive	Pressure
[515]	Ag	–	Air oven	Paper	105	Conductive	Pressure
Gravure printing							
[315]	Ag	water	(poly(vinyl butyral)), PVB	PET	150, 1 min	Conductive	Sweat Sensor
[159]	Ag NP	Ethanol	–	PET	–	Conductive	Humidity

TABLE 4

Selected examples of printable composite inks and their physiological parameter monitoring wearable sensor applications.

Ref	Functional inks	Solvent	Binders/cross linker	Substrate	Curing temp (°C)	Ink property	Sensing application
Inkjet printing							
[517]	PEDOT:rGO-PEI/Au NP	Organic solvent	Thermally annealed	PET	180, 130 s	Conductive	Humidity
[518]	SPS:PEDOT NP/RGO	Organic solvent	Thermally annealed	PET	180, 130 s	Conductive	Humidity
Screen printing							
[519]	CNT + PEDOT:PSS	–	–	PE	70	Conductive	Temperature
	CNT + AgNP			PET	130		Strain
[520]	C + Polymer		Rubber and PE modified polystyrene	PET	120, 20 min	Conductive	Temperature

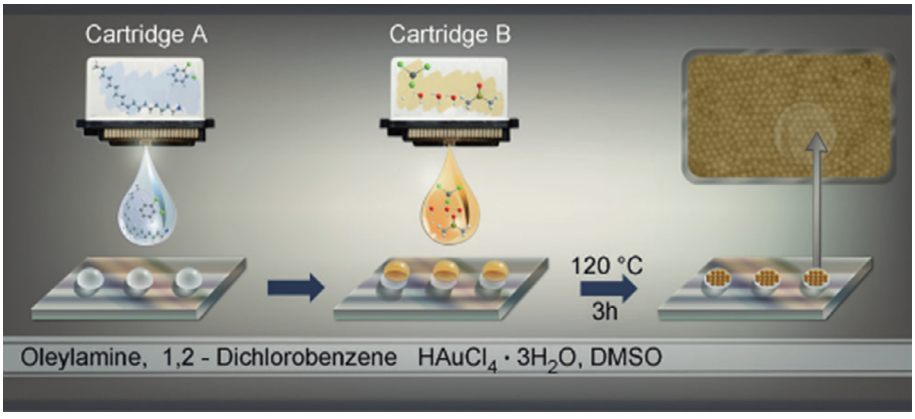

FIGURE 10

Reactive ink synthesis. A schematic demonstration of Au NPs synthesis through reactive inkjet technique (Reprinted from the Ref. [525] Copyright © 2014 WILEY-VCH Verlag GmbH & Co. KGaA, Weinheim).

on-demand facile integration of NPs into various active and passive devices.

As an example, Li et al. have directly printed Cu lines on the paper substrate by reactive inkjet printing method, using Cu as the precursor with aqueous solutions of Cu citrate and sodium borohydride ($NaBH_4$), as reducing reactant/agent. The Cu salt was printed first. Then the reducing reactant subsequently printed from a multi-color print head. At room temperature, the measured conductivity attained on a paper substrate, 1.8×10^6 S/m, is ~1/30 of bulk Cu metal, 59.6×10^6 S/m) [526]. Another example is the synthesis of self-assembled AuNPs with acceptable size uniformity, with diameters as small as 8 ± 2 nm, directly on the substrate using inkjet printing and a unique solvent/precursor system [525]. Walker and Lewis developed room temperature transparent, stable, low viscous and particle-free reactive inks that composed of Ag for producing structures with high conductivities (>10^4 S cm^{-1}).

In PEs devices, the high temperature sintering limits the substrates selection because most flexible polymer substrates are thermoplastic materials with a lower Tg (glass transition temperature), and hence the temperature above that will lead to deformation of the substrate. Patterns printed using MOD inks are electrically insulated until sintered above 150 °C to decompose metal into conductive elemental metal. Many studies are therefore focusing on developing new methods to reduce the sintering temperature for MOD inks.

Curing/sintering

The sintering of metallic nanoparticles is essential to remove the oxides from the substrate surface and conjoining of the metallic particles through focused heating and melting. The sintering improves the electrical performance (conductivity) and microstructure of the printed tracks [527]. Thermal energy [528], non-thermal chemical process [529], pressure assisted [528], or mechanical [530] and several other sintering techniques have been used for sintering of the printed structures depending upon the conductive ink material and substrate material [531–536]. Traditional thermal sintering is not feasible as polymers with low glass transition temperatures are used as substrate to fabricate printed electronics and wearables. Laser and intense pulsed light (IPL) sintering are widely used for sintering of inkjet printed nanoparticles [537,538]. In laser sintering, laser beam is focused on a small area of the printed track and localized thermal energy is provided to exposed area equal to beam spot size (typically several mm diameter). However, in IPL technique, a xenon flash lamp is used and the light is exposed over a large substrate typically several cm^2 area. Therefore, for large area electronics and related printed techniques (*e.g.* R2R), IPL is preferred. Another difference is provision of 'grayscaling' in laser sintering as the laser power can be varied during the exposure of a patterned surface. By controlling the laser intensity, the sintering can be controlled and patterned tracks with varied conductivity can be produced. Nittynen et al. tested and compared plasma, laser and photonic sintering of Ag nanoparticles tracks printed with inkjet printing [539]. The maximum reduction in resistivity of the printed tracks achieved was 15 μΩ cm for plasma sintering, 4.6 μΩ cm for laser sintering and 3.3 μΩ cm for photonic sintering. It was also observed that the microstructure of tracks after photonic sintering was more uniform and comparatively denser than laser or plasma sintering. The significant improvements in the microstructure also corresponds to better mechanical performance.

Substrates

The widely used polymer substrates in PEs application are polyether imide (PEI), PC, poly acrylate (Pacr), PI, polyethylene (PE), polyurethane (PU) and PET [523,540,541]. Among these substrates, PET [542,543], PC [544], and PU [545,546] exhibit an excellent deformability and optical transparencies. Another, popular substrate to integrate sensitive nanomaterials for PEs is polydimethylsiloxane (PDMS) films due to its excellent elasticity and biocompatibility [29,30,547,548]. For most PEs, low porosity and high surface energy flexible substrates are preferred. For all applications, heat resistance, dimensional stability and gas-impermeability are the major requirements for flexible substrates. Fabrication of flexible devices involves different processing steps that require high temperature of at least 300 °C, therefore, heat resistance is a key requirement to withstand high processing temperatures. The substrate selection for a particular device manufacturing must meet physical, mechanical, chemical, thermal and optical requirements, as well as, compatibility with the conductive inks are also important. Different polymers used as flexible substrates and their properties are listed in Table 5 and Fig. 11 shows the screen printed strain sensor on different flexible substrates.

In addition to these polymer substrates, cellulose paper and textiles (*e.g.,* silk, cotton, etc.) are explored and developed as substrate materials for flexible sensor devices. Textile is one of the generally used and inexpensive flexible material and the studies of wearable sensors incorporation in textiles has been on-going since the 1980s [560]. The textile substrates are renewable and friendly to the body skin. They are offering many opportunities for deploying sensors [561,562], energy harvesting device [563], field effect transistors [564], and antennas, [565], which are potential for smart textiles/garments. The combination of electronic and textile technologies in particular can be useful in different applications, for instance to detect the physical parameters of patients or to increase the safety level of people who work in dangerous environments, by monitoring their physiological parameters [566,567]. Sensors integrated or woven into textiles for monitoring body temperature [568], heart rate [569], respiration [570], and humidity [511] using inkjet printing technique have been demonstrated. Now, conductive fabrics have been advanced in different clothing, including gloves [571,572], shirts [573,574] and socks [575].

Interestingly, Mattana et al. have developed humidity and temperature sensors on Kapton flexible foils (PI sheets, 50 μm-thick, provided by DuPont) and integrated into textiles [511]. In their study, thin-film meander resistor that is sensitive to temperature and thin film interdigitated capacitive transducer that is sensitive to humidity are the sensing elements. They have inkjet printed the ink based on AgNP on the PI substrate. Both the developed temperature and humidity sensors were integrated into the garment. Conductive yarns are used in the garment to create contact with these sensors. The developed temperature sensor has been operated with a sensitivity of 5 °C at a

TABLE 5

Various polymer substrates and their properties [216,219,544,549–558].

Flexible Polymer substrates	Surface energy (mN/m)	Transparency (%)	Water abso. (%)	Dimensio. Stability	Surface roughness	Solve. resist.	Tg (°C)	Modulus (M pa)
Polyethylene Terephthalate (PET)	44.0	90	0.6	Good	Poor	Good	70–110	2–4.1 $\times 10^3$
Polycarbonate (PC)	34.2	92	0.16–0.35	Fair	Good	Poor	145	2.0–2.6 $\times 10^3$
Polyurethane (PU)	38	–	0.2	Good		Good	80	7
Polyimide (PI)	43.8	35–60	1.3–3.0	Fair	Good	Good	155–270	2.5 $\times 10^3$
Polydimethylsiloxane (PDMS)	20.4	–	>0.1	Good		Poor	125	1
Polypropelene (PP)	30.2	84.0–90.0	0.01	Good	Good	Good	0	0.008–8.25 $\times 10^3$
Polyacrylate (Pacr)	–	>90	0.2	Good	Fair	Good	105	2.4–3.4 $\times 10^3$
Polyethlene Naphthalate (PEN)	–	88	0.3–0.4	Good	Good	Good	118	0.1–0.5 $\times 10^3$
Polyethersulphone (PES)	–	89.0	1.4	Fair	Good	Poor	223	2.2 $\times 10^3$
Polycyclic Olefin (PCO)/Poly-norbonene (PNB)	–	91.6	0.03	Good	Poor	Good	35	1.9 $\times 10^3$

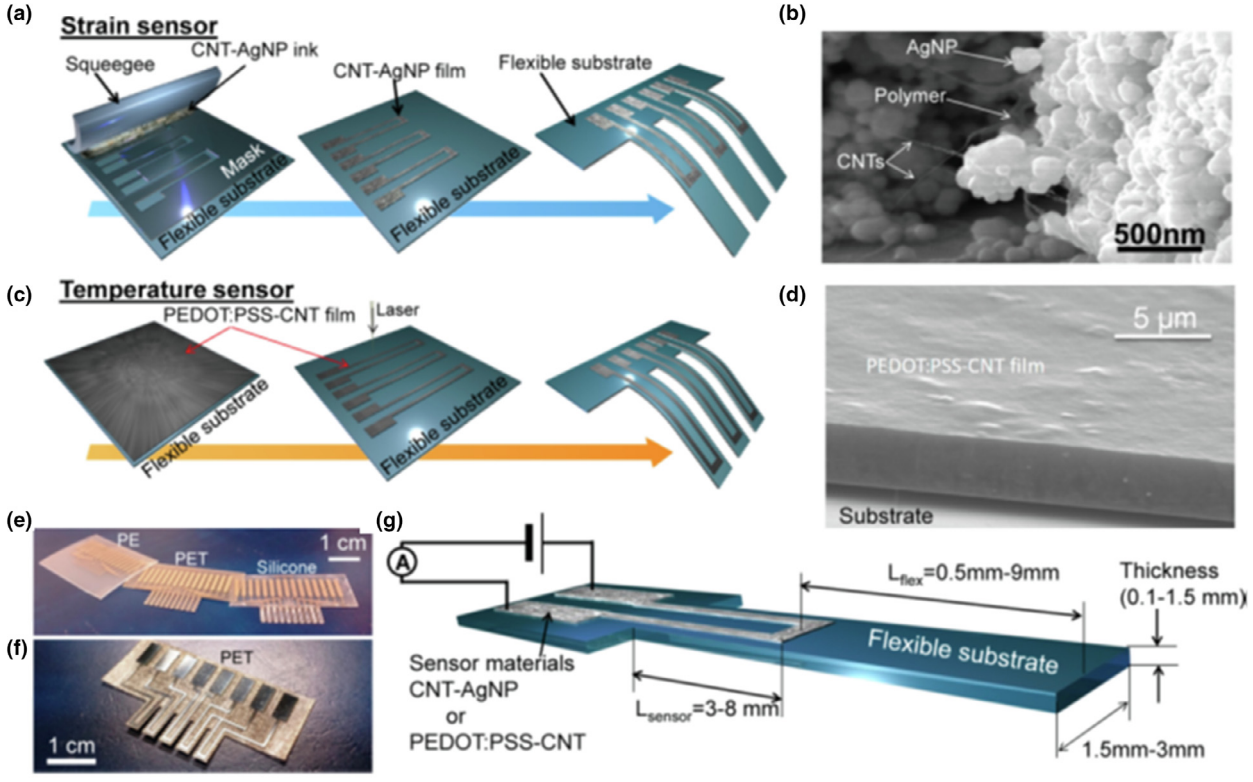

FIGURE 11

Screen printed strain sensor and its characterization. (a) Schematic of screen printed strain sensor. (b) SEM picture of printed composite CNT-AgNP film. (c) Schematic of making temperature sensor using a laser cutter. (d) SEM picture of PEDOT: PSS-CNT film. (e) Picture of strain sensor array on printed on a silicone, a PET and a PE. (f) Photo of temperature sensor array on a PET. (g) Schematic of device for characterization (Reprinted from the Ref. [559], Copyright © 2014, American Chemical Society).

temperature range 10–80 °C and the detection range of the humidity sensor with 10% sensitivity is 25–85%.

For obtaining highly sensitive pressure sensors in textile, it is important to use fabrics having huge surface roughness and excellent electric conductivities. Different materials including metal NWs and NPs (*e.g.,* Ag NWs and Ag NPs) [577,578], conductive organic polymer (*e.g.,* PEDOT) [579] in combination of fabrics/fibers and nanomaterials based on carbon (*e.g.*, rGO and CNTs) [580,581], have been demonstrated for manufacturing textile based pressure sensors. Recently, Ziqiang Zhou et al. have

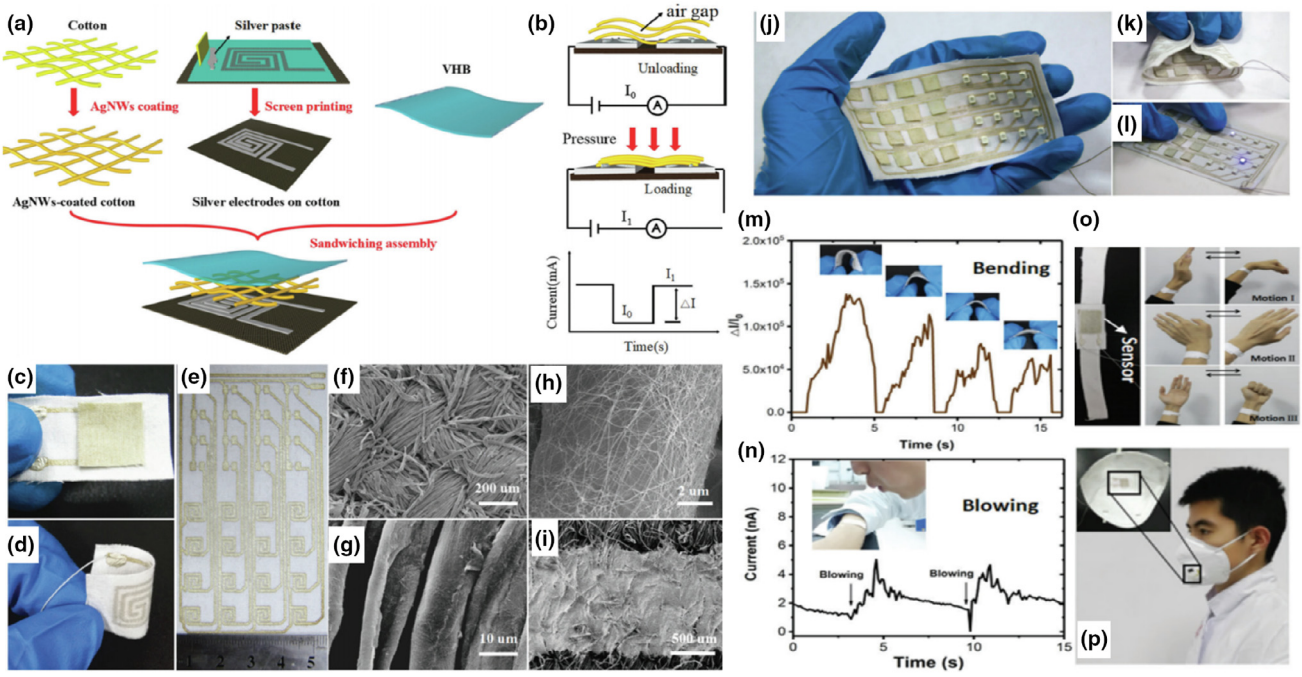

FIGURE 12

Inkjet printed pressure sensor and application. Schematic demonstration of (a) pressure sensor integration on fabrics and (b) its operating mechanisms. (c) and (d) Images of pressure sensors and (e) its mass scale production on a cotton. SEM images of (f)–(h) cotton fibers coated with Ag NW (i) Ag-printed electrode on cotton. (j) and (k) Pictures of LED and pressure sensor arrays integrated on a garment. (l) Photo shows the LED brightness by pressing arrays of pressure sensors. (m) Optical textures and the current signal with respect to different bending angles. (n) Optical image of wind blowing using mouth and the detection of current. (o) Image showing different wrist movements after wraping the sensor. (p) The device connected to the mask (Reprinted from the Ref. [576], Copyright © 2018, Royal Society of Chemistry).

developed all-fabric supersensitive piezoresistive pressure sensor for monitoring movements of human by using textile based screen printed Ag paste electrode arrays (Fig. 12) [576]. This manufacturing process is simple, cost effective and appropriate for mass scale integrated fabrication. Different motions of hand including wrist bending, hand waving etc. (Fig. 10o) and a changes in the frequency of respiration can be monitored accurately (Fig. 10p) by using its wearable bracelet form.

Recently, paper substrate has shown a great promise in developing physiological parameter monitoring sensors due to its availability, flexibility and recyclability. Various applications of the cellulose based electronic devices are, sensors [582,583], generators [584,585], transistors [586–588], diodes [589] and energy storage devices [582,590,591]. For using paper substrate in PEs, the use of low processing temperatures (≤150 °C) are important as it degrade easily at higher temperatures. Wearable vital parameter monitoring sensors have been developed based on these paper substrates. For example, wearable pressure sensor device based on ultrathin Au NW has been developed by direct coating of Au NWs on a Kimberly-Clark tissue paper [515]. The response time of this sensor shows <17 ms and it detected 13 Pa pressure with a sensitivity >1.14 k/Pa.

Another example is the development of 3.5 cm × 2.5 cm sized multisensory paper watch based physiological parameters monitoring device (Fig. 13a and b) [592]. Using this lightweight multisensory cost effective and recyclable device simultaneous and continuous monitoring of temperarure, skin humidity and pressure (Fig. 13) is possible. They have encapsulated fully in a 3D printed flexible wristband. Within this device the sensor monitoring for pressure contains a capacitive parallel plate structure and the temperature sensor is with resistive structure whereas, humidity sensor uses a capacitive structure through interdigitated electrodes design. They have used Ag ink for drawing the conductive patterns.

In one of the latest effort, Chen et al., developed cellulose paper based pressure sensor using screen-printing technique (Fig. 14a) [593]. In their work, flat printing paper was used as a flexible pressure sensor substrate and the carbonized crepe paper (CCP) as the active material. This CCP is highly conductive. The interdigital electrodes were screen-printed using Ag paste. The developed CCP based flexible pressure sensor shows sensitivity greater than 2.52 k/Pa, broad applicable range of pressure (0–20 kPa), fast speed (<30 ms), lower monitoring limit (~0.9 Pa), and great durability (>3000 cycles). These properties enable the fabricated CCP based pressure sensor to be able to sense pressure variation caused by wrist pulse, respiration, phonation, etc. and to monitor spatial pressure distribution in real time as the pixelated array (Fig. 14b and c). The sensing mechanism of this CCP pressure sensor is the pressure dependent contact within the CCP and between the CCP and interdigitated electrodes.

Power management and storage

Along with the rapid advances of high performance flexible wearable electronics, there is an ever-growing demand for light-weight, flexible power sources and storage devices today [594–596]. Several methods have been demonstarted to produce

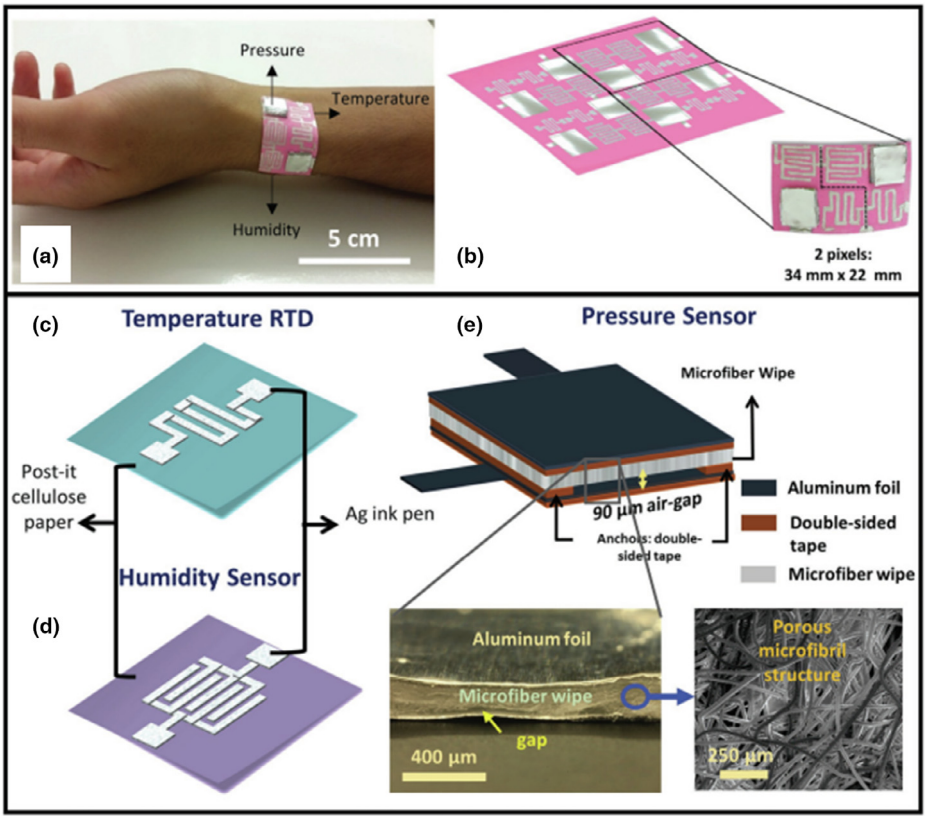

FIGURE 13

Health monitoring paper based patch. (a) Picture of the multifunctional paper-based sensors for temperaure, body humidity and pressure monitoring. (b)–(e) Schematics of the multisensory pattern, temperature sesor, humidity sensor and pressure sensor (Reprinted from the Ref. [592], Copyright © 2017 WILEY-VCH Verlag GmbH & Co. KGaA, Weinheim).

compliant flexible batteries. Since the flexible wearables are free of external electrical connections, light weighted and highly integrated, self-powered flexible PEs possessing excellent coordination among energy harvesting, storage and management, are highly preferred. Flexible batteries play a key role in achieving wearables and compatible electronics. Several approaches are required for powering wearable PEs from the development of innovative materials for faster charging, and for development of smaller and more energy efficient batteries to improve the existing energy storage device efficiency. The lithium-ion batteries [623] and supercapacitors [658] are the existing flexible energy storage devices. Even though sensing elements with self-powering mechanisms have been reported recently [53,597–600], most of the health detecting systems need power for driving sensing components. In addition to that, power is essential to collect the data, analysis the data and for giving feedback. Data retrieved from multiple sensors in a wearable is becoming much more complex to manage. As more sensors are added to wearables, more power is needed to run sensor data and turn it into useful information. In wearable systems, the primary role of the power source is to offer required power. This power souce should be placed closer to the sensor module for minimizing the usage of wires and related problems such as complexity of the device, discomfort and losses due to the resistivity. Next important requirements are longer battery life and sufficiently safe materials and safeguards. In wearable devices, flexible battery constructs with high performances and energy management systems are key design components [601–611]. Coupling flexible devices with power sources that are also flexible, is very challenging.

Lithium-ion batteries (LIBs)

Flexible lithium-ion batteries (LIBs) (Fig. 15) are very versatile storage systems for PEs devices, since this is inexpensive and offering much span of life, and large energy density [612–616]. The main components of conventional LIBs are a cathode, anode, lithium salt electrolyte, separator (made up of polymer) and its packaging [617]. The electrodes (also called active materials) that are used for LIB must have high capacity and low self-discharge. Battery performances mainly depends on the active materials used for fabricating the cathode and anode. Numerous electrodes that normally consist of soft inorganic or organic materials in flexible substrates have been developed for configuring flexible LIBs. Flexible solid polymer materials and different functional materials have been proposed [659,660] as electrolytes and electrodes. 1D materials have great potential to be fabricated as the flexible and transparent electrode due to great electrical and mechanical properties [619,620]. For the realization of highly flexible LIBs, widely used coin type LIBs are not appropriate [618]. Flexible LIBs require the development of flexible anodes, cathodes, electrolytes and separators. Flexible cathode and anode materials exhibiting excellent performances are

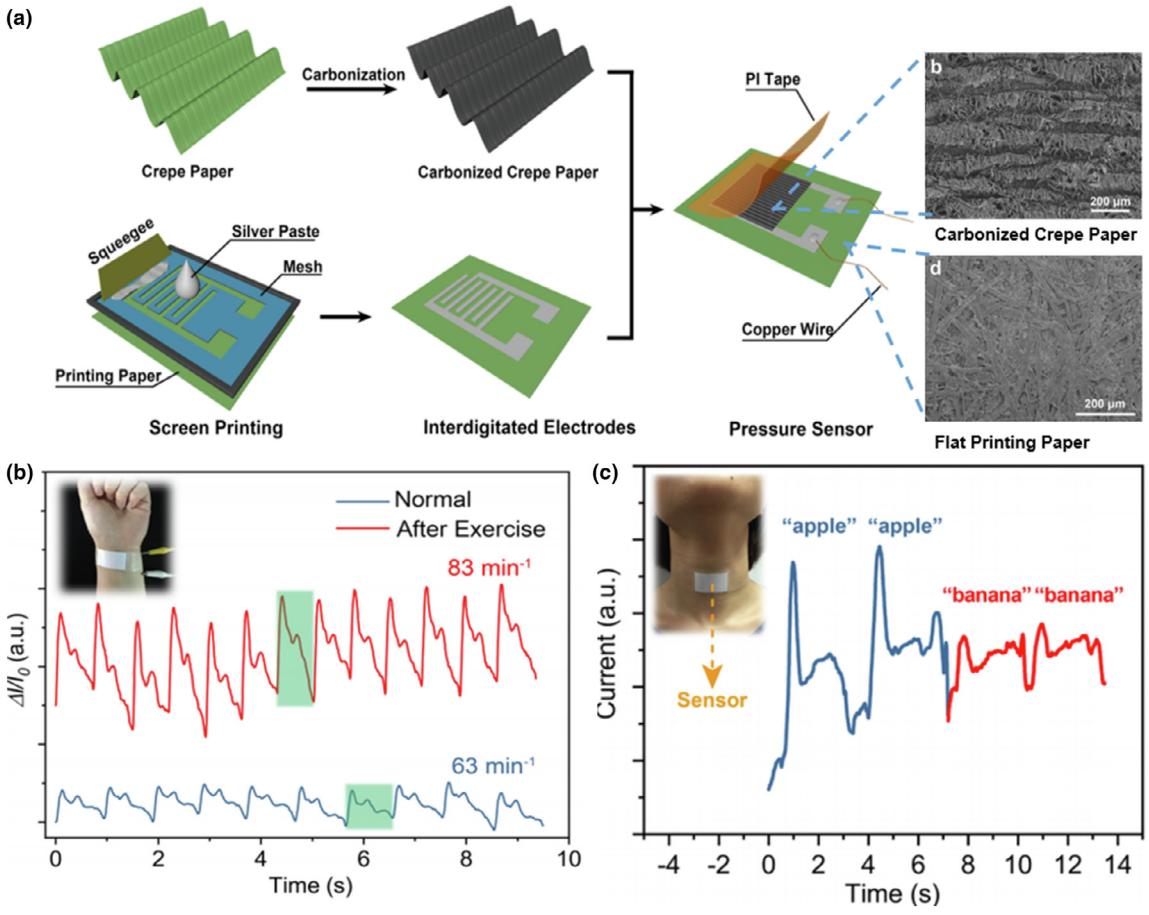

FIGURE 14

Scematic of paper based pressure fabrication and its applications. (a) Schematic demonstartion of the production of pressure sensor based on carbonized crepe paper (CCP). (b) Wearable CCP based pressure sensor application to detect wrist pulse and (c) sensor current changes by phonation of the words "apple" and "banana" (Reprinted from the Ref. [593], Copyright © 2018, American Chemical Society).

need to be used for manufacturing flexible power storage systems. The development of new active materials for electrodes with highly improved electrochemical and mechanical performances is a big challenge for producing completely flexible LIBs. The provision of high levels of safety under repeated mechanical deformation is also a challenge. In recent years, various structural designs (Fig. 15a–c) and manufacturing techniques (Fig. 15g–j) for flexible LIBs have been developed [616,661–667]. Numerous flexible LIBs have been developed [616,621–625]. LIB electrodes have been successfully developed using inkjet [661,662], screen [663,664] and 3D [667] printing processes. The printing processes enables achiving inexpensive, thinner and lighter LIBs, compared to conventional methods.

Interestingly, Qian et al., developed a spine-like highly flexible and mechanically stable LIB with remarkable electrochemical performances, inspired by the shape of the natural vertebrate spine for flexible and wearable electronics (Fig. 16) [171]. They have used commercially available $LiCoO_2$ (MTI Corp.) as cathode and graphite (MTI Corp) as anode. The energy density of this class of flexible battery was found to be over 85% of that in conventional packing. Compared to the previous reports [590,614,615,626,627], this developed battery is highly stable.

In another example, a coaxial, flexible LIB with a shape of fiber was developed by using CNT/Si composite yarns (as anode) onto a cotton fiber (Fig. 17a–e) [628]. In a separate study, batteries having stretching properties with an integrated recharging wireless mechanisms (Fig. 17f–n) have been reported [629]. In this study they have used $LiCoO_2$ as cathode, $Li_4Ti_5O_{12}$ as anode, gel electrolyte (which is a combination PE oxide, lithium perchlorate, dimethylcarbonate and ethylene carbonate) and silicone elastomer substrate. For depositing cathode and anode materials, the transfer printing technique was performed. Another study showed the fabrication of a full graphite/$LiFePO_4$ (carbon-coated lithium iron phosphate) LIB based on paper substrate [630]. This highly flexible battery shows a total specific energy density 188 mWh/g of full paper battery at C/10.

Significant developements have been achieved on the structure designing and manufacturing of LIBs with high flexibility over the last years. However, for the practical application in PE flexible devices, there are many problems to be resolved *i.e.*, optimization of the packaging materials, current collectors, electrodes, and electrolytes.

Flexible super capacitors

Flexible and printable super capacitors are considered as potential candidate for meeting challenges of energy storage for wearables [631]. For printed super capacitors, various methods including screen printing, inkjet printing, and R2R printing

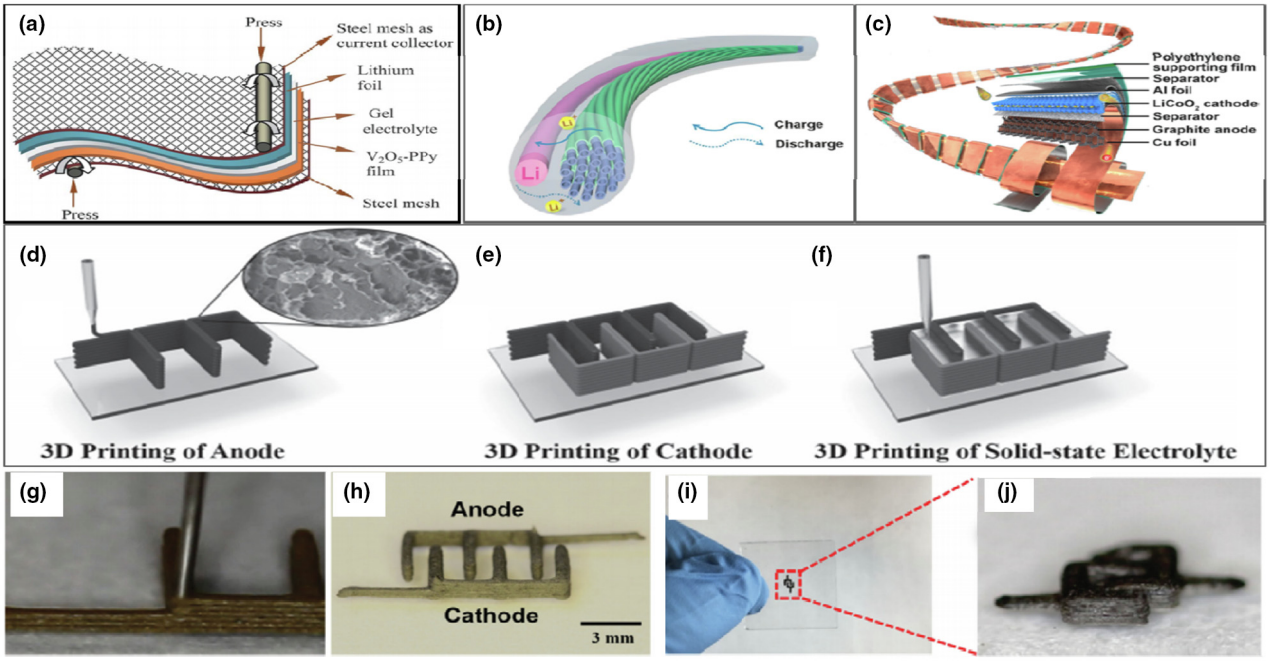

FIGURE 15

(a) Schematic demonstration of a fully flexible Lithium-Ion Battery (LIB). (Reprinted from the Ref. [616], Copyright © 2012 Royal Society of Chemistry.) (b) Schematic of a wire like structure of LIB. (c) The schematic illustration of a spine-like battery. (b and c Reprinted from the Ref. [666], Copyright © 2019, American Chemical Society). (d–f) Schematic of interdigitated electrodes 3D printed. (g) Photograph of syringe loaded with inks (lithium ion phosphate/graphene oxide ink) and (lithium titanium oxide/graphene oxide ink). (h) 3D printed interdigitated cathode and anode. (i and j) Photograph of miniaturized 3D-printed electrodes. (d–j Reprinted from the Ref. [667], Copyright © 2016 WILEY-VCH Verlag GmbH & Co. KGaA, Weinheim.)

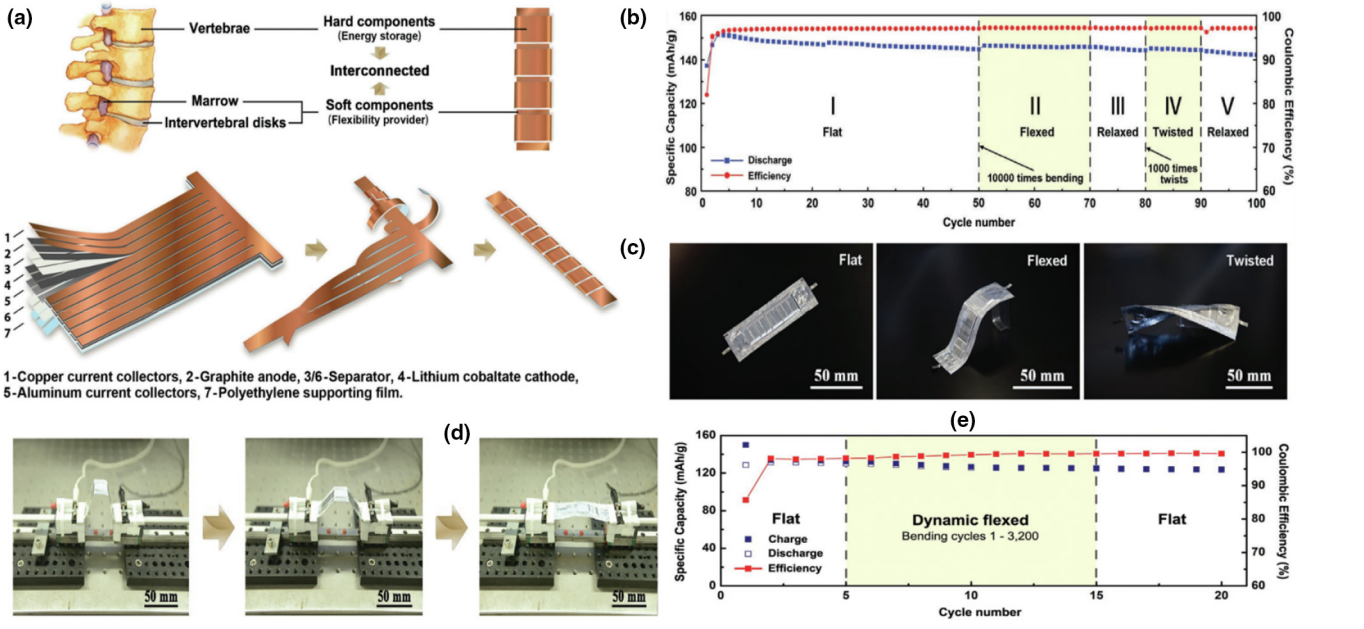

FIGURE 16

Bioinspired spine like battery and its characterization. (a) Schematics of bio inspired spine like battery structure and fabrication process. (b) Charge or discharge cycle test. (c) Optical images of battery curresponding to the figure b. (d) Pictures of spine like battery in different states. (e) is the cycling performance under repetitive mechanical load test curresponding to the figure (d). (Reprinted from the Ref. [171], Copyright © 2018 WILEY-VCH Verlag GmbH & Co. KGaA, Weinheim.)

techniques have been used. The printed flexible super capacitors are composed of substrates, electrolytes, current collectors, and active materials. The inks that are suitable for these capacitors are classified as current collector, active material and electrolyte inks. In a very recent study, solid state super capacitors have been screen printed using Ag@PPy ink over a flexible PET substrate,

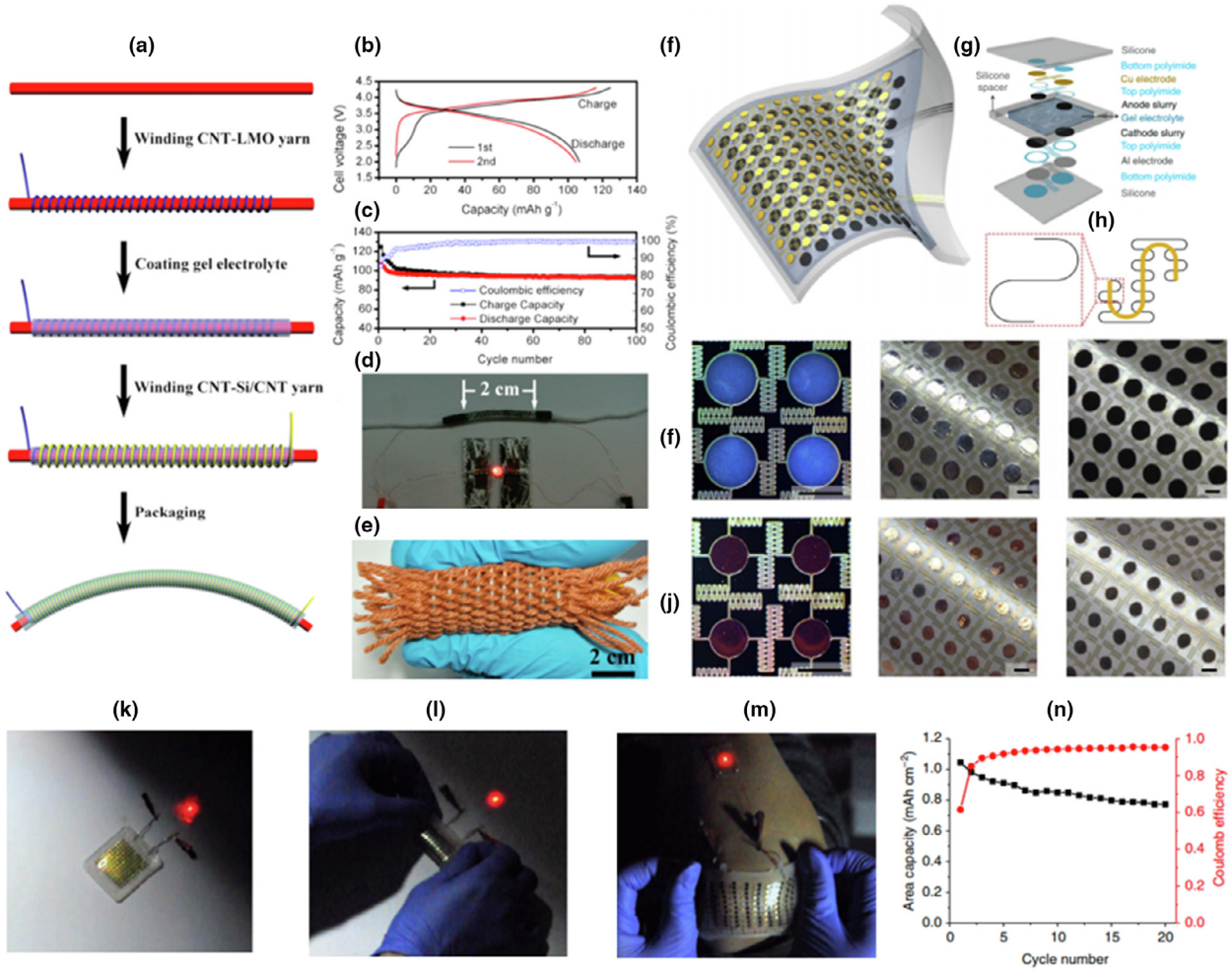

FIGURE 17

Fiber LIB fabrication, characterization and application. (a) Schematic demonstartion of coaxial fiber LIB fabrication (red color = cotton fiber, blue color = CNTLMO composite yarn and yellow color = CNT-Si/CNT composite yarn). (b) and (c) are the LIBs voltage profiles and span of life between 2.0 and 4.3 V at 1C. (d) Picture of a fiber LIB to lighten up a LED. (e) Fiber LIBs in a garment. (a–e Reprinted from the Ref. [628], Copyright © 2014, American Chemical Society). (f) Schematic demonstration of stretching and bending of a completed device. (g) Battery design with the layout of different states. (h) Demonstration of serpentine geometries as interconnects. Pictures of (i) aluminium and (j) Cu electrodes and interconnects on silicon substrates. Scale bar in (i) and (j) are 2 mm. (k)–(m) Electrochemical and mechanical properties. (n) Capacity retention and coulombic efficiency over a number of cycles. (f–n Reprinted from the Ref. [629], Copyright © 2013, Springer Nature.)

which provides energy as high as 4.33 μWh/cm^2 and shows higher mechanical flexibility [632]. In an earlier study, Kristy et al. developed screen printed and knitted super capacitors on garments with a capacitance as high as 0.51 F/cm^2 and high flexibility (Fig. 18a–f) [633]. In another work, asymmetric all-printed super capacitors on garments having energy 0.0337 mWh/cm^2 have been developed [634].

Similarly, inkjet-printed in-plane super capacitors have been developed. The paper based in-plane solid state super capacitor has been inkjet printed in one of study using SWNTs/ACs (single-walled carbon nanotubes/active rbons) current collectors (Fig. 18g) [635]. These highly flexible capacitors were produced by a sealing treatment having capacitance 100 mF/cm^2. Recently, a transparent (71% transmittance) and flexible in-plane super capacitor having 99 μF/cm^2 capacitance was demonstrated using inkjet printing method (Fig. 18h–j) [637]. Another report explains the development of flexible and cost effective paper based inkjet printed super capacitors, exhibiting 1.586 F/cm^2 capacitance and 22 mWh/cm^3 energy density (at a power density of 0.099 W/cm^3) [638]. In 2015, Lee et al. developed R2R printed flexible super capacitors by patterning AgNP and active carbon electrodes on a polymer substrate. This shows 45 mF/cm^2 capacitance, 4.1 μWh/cm^2 energy density and excellent flexibility [636]. In a separate work, very recently, Kang et al. have obtained R2R laser-printed super capacitors, exhibiting excellent performance, using the electrodes made up of graphene-graphitic carbon [639]. In a latest work, Zhang et al., inkjet printed micro-supercapacitors on AlO_x-coated PET and paper substrates using MXene (transition metal (M) carbides and nitrides (X)) organic inks with high printing efficiency and spatial uniformity (Fig. 19) [640]. The Z values (2.2–2.6) of used MXene organic inks are within the optimal value range for stable jetting, $1 < Z < 14$. They have tuned thickness and sheet resistance R_s of the printed patterns by adjusting the printing pass (Fig. 19d). They report

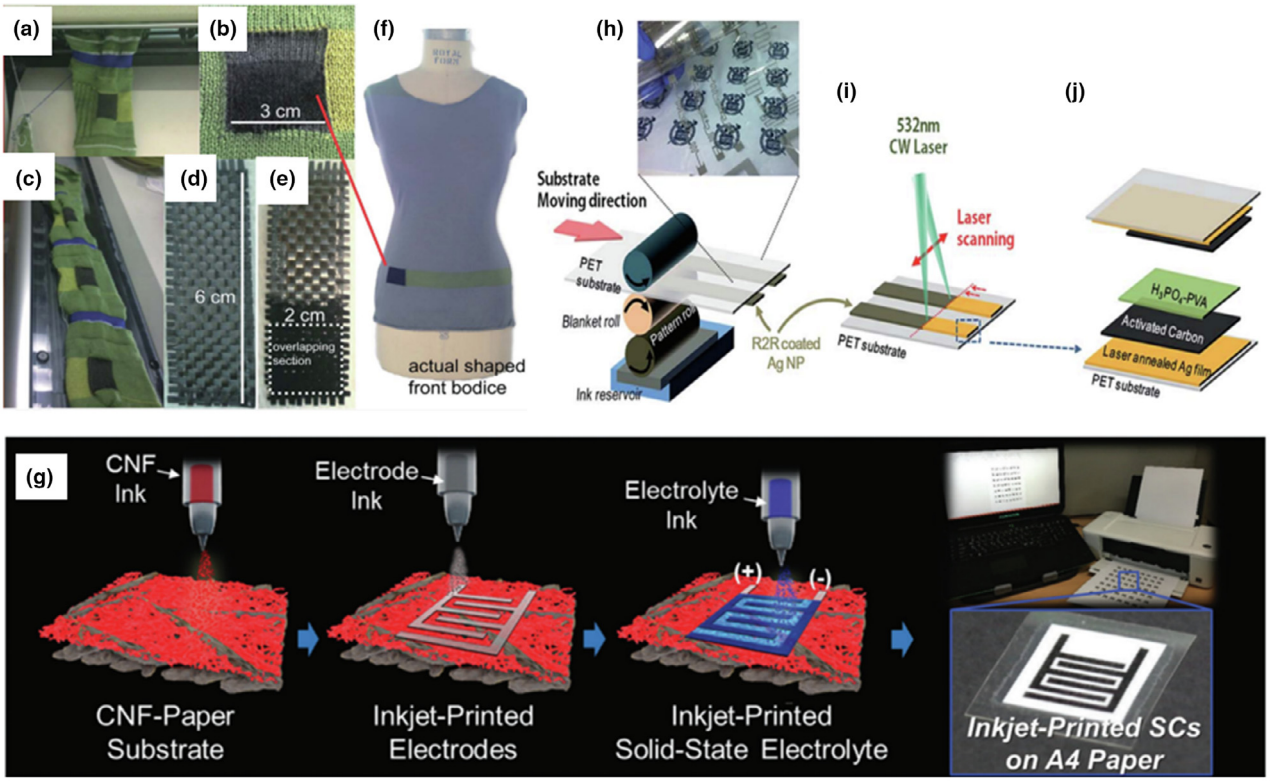

FIGURE 18

(a)–(f) Screen printed super capacitor embedded in textile. (a–f Reprinted from the Ref. [633], Copyright © 2013, Royal Society of Chemistry.) (g) Manufacturing states of paper based in-plane super capacitors using inkjet printing method (Reprinted from the Ref. [635], Copyright © 2016, Royal Society of Chemistry). (h)–(j) Fabrication process of R2R printed super capacitors and its explanation. (a–f Reprinted from the Ref. [636], Copyright © 2015, Royal Society of Chemistry.)

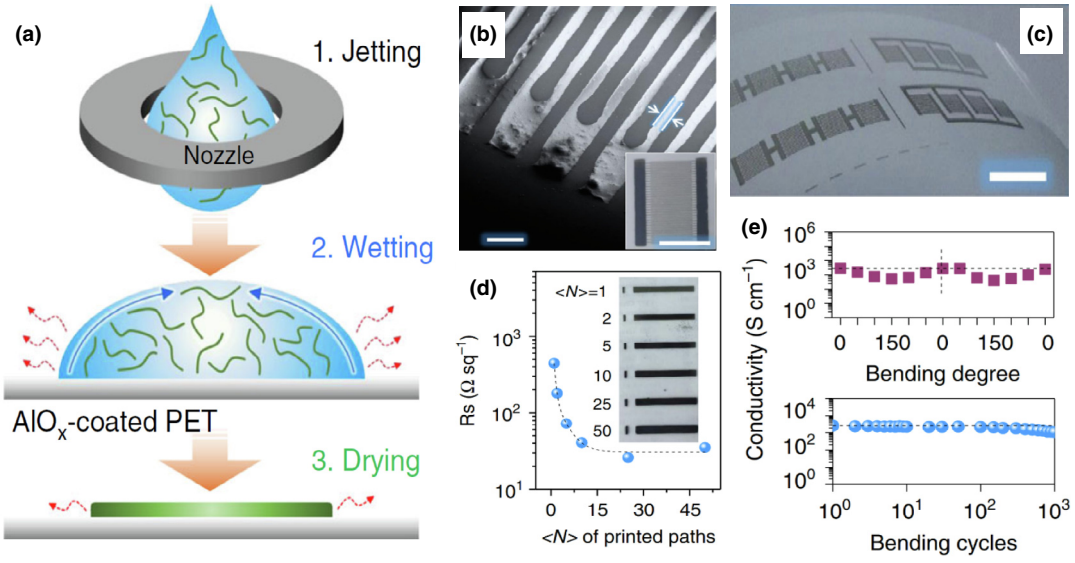

FIGURE 19

Inkjet printed microsupercapacitors. (a) Schematic of fine resolution of inkjet printing of MXene organic inks on PET substrate; the curved green lines indicates MXene nanosheets and blue and red arrows shows the droplets inward and outward flows. (b) Scanning Electron Microscopic (SEM) image of the inkjet printed microsupercapacitor. Inset shows the whole device. (c) Inkjet printed microsupercapacitors on PET substrate. (d) The sheet resistance plotted *vs* number of passes, <*N*> (optical images of various printed lines (2 cm in length) with different <*N*> is given as inset). (e) The electronic conductivity as a function of bending degree and number of bending cycles. (Reprinted from the Ref. [640], Copyright © 2019, Springer Nature.)

that the volumetric capacitance (up to 562 F/cm^3) and energy density (as high as 0.32 μWh/cm^2) of the all-MXene printed micro-supercapacitors are orders of magnitude greater than existing inkjet/extrusion-printed active materials [641–643].

Conclusions and future perspectives

In this paper, the current state-of-the-art of the materials and manufacturing methods for large area flexible electronics and wearables for healthcare applications are highlighted. The requirements to print high resolution and highly conductive tracks on lightweight and range of flexible substrates resulted in the development of contact and non-contact printing techniques in R2R and S2S production. Although R2R printing provide inexpensive high throughput large volume printed electronics solution, the capital costs are high for R2R production unit. Therefore, small scale companies are pushed towards sheet feed processing techniques. Nevertheless, most of the printed electronics production techniques are suitable for both mechanisms. A good range of printing techniques including gravure, flexography, inkjet and screen printing are developed that covers high throughput and good resolution from submicron to 100-micron resolution. Some techniques (such as screen printing) require multiple print cycle, thus provide low throughput. Gravure technique although provide scalable solution for PE, reliability and repetition in resolution quality are still challenging. Therefore, state of the art metrology tools is needed to examine the printed circuits and provide feedback to the printer in case of defect occurrence.

There is a strong and pressing demand for the development of multiple sensor-integrated small wearable form factor with robust control of data storage, communication and power supply for real time feedback from multiple physiological conditions. Devices currently available are large and have limited functionalities such as the low level of comfort and body conformability, high production costs and require very specific on-body placement (*e.g.* ECG and EMG) for accurate monitoring. The physical packaging of multiple components into the flexible form factor and its manufacturability is very challenging because of the diversity in the parts with different mechanical and electrical properties. The rigid form factors of component devices (sensors, battery, transmission circuit, Bluetooth *etc.*) restrict placement of devices on human body. The advanced production technologies in PE enable use of flexible substrates to print electronic components, suitable for on-body placement with higher level of comfort and easiness. This includes the design and production of flexible storage devices with a power provision capacity and low power circuit consumption while achieving low thickness, high sensitivity, high resolutions, high robustness, and long life times, in a sustainable and low cost manner. Reliability of the sensors throughout the life time without need of calibration and the battery life of wearables are critical concerns when it comes to the mass markets. These factors remain challenging as the accuracy of the sensors have high error bars in the majority of wearable sensor devices and the batteries do not last a satisfactory amount of time, and still need to be charged on almost a daily basis. Therefore, to exploit the potential of wearable sensor systems, the development and integration of high precision sensing devices with the latest battery technology are required. The enormous data generated by the sensor devices, limited storage and real time feedback require continuous transfer of data from wearable device to cloud storage which utilize significant amount of energy. Therefore, data management strategies are important and developed to ensure low use of battery energy for data transfer without losing crucial data for specific application.

It is expected that with attention to key challenges discussed above, in developing a new vision, we need also to focus on the use of sustainable and recyclable materials; using more cost effective and abundant available materials for inks and substrates and techniques with large volume production capabilities. Achieving an uncomplicated printability without the use of high amount of additives, stabilizers free NP inks, and low temperature cured precursor inks, offers huge technological significance. The major factors influencing the growth in wearable sensor devices include that they are smaller, smarter, cheaper, require less energy and they integrate with an external device (such as a mobile phone and/tablet) for real-time monitoring. The large amount of sensed data generated using wearable systems has to be managed and processed to extract relevant information. This data is processed and displayed as an integral part of the wearable sensor monitoring systems. For that, the development of adavanced software for recording and displaying combined signals from wearables and provision of feedback to the user is needed. Improved reliability convenience, and accuracy, lower cost and the supportive set-up for the assistance and monitoring need to be developed to bring the developments reviewed herein closer to mainstream usage and commercialization. To reduce defects and scrap and ensure high quality of the sensor production, optical, electrical, and high speed camera based online metrology tools need to be employed. With all these, a flexible and replaceable power source with a long life time is important. To meet the future flexible cutting-edge PEs demand, it is necessary to develop low cost, flexible, light-weight, and sustainable energy storage systems with high power and energy density. These are the key drivers of the future competitiveness of the flexible and wearable electronics industry.

Acknowledgments

This research is supported in part by a research grant from Science Foundation Ireland (SFI) under Grant Number 16/RC/3872 and is co-funded under the European Regional Development Fund and by I-Form industry partners.

References

[1] M. Ha et al., ACS Nano 9 (4) (2015) 3421.
[2] M. Amjadi et al., Adv. Funct. Mater. 26 (11) (2016) 1678.
[3] X. Wang et al., Adv. Sci. 2 (10) (2015) 1500169.
[4] T.Q. Trung, N.-E. Lee, Adv. Mater. 28 (22) (2016) 4338.
[5] W. Zeng et al., Adv. Mater. 26 (31) (2014) 5310.
[6] M.L. Hammock et al., Adv. Mater. 25 (42) (2013) 5997.
[7] S. Xu et al., Science 344 (6179) (2014) 70.
[8] T. Martin, E. Jovanov, D. Raskovic, in: Proceedings of the 4th International Symposium on Wearable Computers 2000 Oct 16-17; Atlanta, GA. p. 43.
[9] U. Anliker et al., IEEE Trans. Inform. Technol. Biomed. 8 (4) (2004) 415.
[10] R.E. Mayagoitia, A.V. Nene, P.H. Veltink, J. Biomech 35 (4) (2002) 537.
[11] M. Chan et al., Artif. Intell. Med 56 (3) (2012) 137.
[12] G. Appelboom et al., Arch. Publ. Health 72 (2014) 28.

[13] H.E. Montgomery-Downs, S.P. Insana, J.A. Bond, Sleep and Breath 16 (3) (2012) 913.
[14] Y. Pang et al., ACS Nano 12 (3) (2018) 2346.
[15] M. Sekine et al., Med. Eng. Phys. 22 (4) (2000) 285.
[16] P.S. Pandian et al., Med. Eng. Phys. 30 (4) (2008) 466.
[17] E. Sardini, M. Serpelloni, Lect. Notes Electr. Eng. 162 (2014) 201.
[18] D. Nagae, A. Mase, Rev. Sci. Instrum. 81 (9) (2010) 094301.
[19] U. Lindemann et al., Med. Biol. Eng. Comput. 43 (5) (2005) 548.
[20] C.-C. Yang, Y.-L. Hsu, Telemed. J. E Health 15 (1) (2009) 62.
[21] C. Beach et al., IEEE Acess 6 (2018) 44010.
[22] L. Viry et al., Adv. Mater. 26 (17) (2014) 2659.
[23] J.-Y. Sun et al., Adv. Mater. 26 (45) (2014) 7608.
[24] D.J. Lipomi et al., Nat. Nanotechnol. 6 (12) (2011) 788.
[25] S. Park et al., Adv. Mater. 26 (43) (2014) 7324.
[26] S. Yao, Y. Zhu, Nanoscale 6 (4) (2014) 2345.
[27] Y. Zang et al., Nat. Commun. 3 (6) (2015) 6269.
[28] C. Pang et al., Adv. Mater. 27 (4) (2015) 634.
[29] G. Schwartz et al., Nat. Commun. 4 (2013) 1859.
[30] S.C.B. Mannsfeld et al., Nat. Mater. 9 (10) (2010) 859.
[31] J. Wang et al., Nanoscale 7 (7) (2015) 2926.
[32] J. Lee et al., Adv. Mater. 27 (15) (2015) 2433.
[33] Y. Joo et al., Adv. Electron. Mater. 3 (2017) 1600455.
[34] C.M. Boutry et al., Adv. Mater. 27 (43) (2015) 6954.
[35] Z. Lei et al., Adv. Mater. 29 (22) (2017) 1700321.
[36] R.C. Webb et al., Nat. Mater. 12 (10) (2013) 938.
[37] C. Yu et al., Appl. Phys. Lett. 95 (2009) 141912.
[38] D.-H. Kim et al., Small 8 (23) (2012) 3263.
[39] S. Gong et al., Nat. Commun. 5 (2014) 3132.
[40] H. Chen et al., Adv. Funct. Mater. 27 (3) (2017) 1604434.
[41] Y. Gao et al., Adv. Mater. 29 (39) (2017) 1701985.
[42] Y. Enokibori, A. Suzuki, H. Mizuno, Y. Shimakami, K. Mase, in: Proceedings of the ACM Conference on Pervasive and Ubiquitous Computing Adjunct Publication, Zurich, Switzerland, 8–12 September 2013.
[43] G. Fadeyev et al., Sens. Actuators, B: Chem. 221 (2015) 879.
[44] Z. Lin et al., ACS Nano 11 (9) (2017) 8830.
[45] T. Li et al., ACS Nano 11 (4) (2017) 3950.
[46] J. Zou et al., Adv. Energy Mater. 8 (2018) 1702671.
[47] M.-F. Lin et al., Nano Energy 44 (2018) 248.
[48] X. Wang et al., Adv. Mater. 29 (15) (2017) 1605817.
[49] J. Chen et al., Nano Energy 33 (2017) 508.
[50] Y. Sun et al., ACS Appl. Mater. Interfaces 9 (50) (2017) 43822.
[51] Q. Zhang et al., Adv. Mater 29 (17) (2017) 1606703.
[52] F. Yi et al., Adv. Funct. Mater. 25 (24) (2015) 3688.
[53] Y.M. Park et al., Nano Convergence 5 (1) (2018) 15.
[54] S. Rossi, C. Mancarella, C. Mocenni, L.D. Torre, IEEE 3rd International Forum on Research and Technologies for Society and Industry (RTSI) 2017.
[55] J.-H. Bahk et al., J. Mater. Chem. C 3 (40) (2015) 10362.
[56] H.-B. Yao et al., Adv. Mater. 25 (46) (2013) 6692.
[57] L. Pan et al., Nat. Commun. 5 (2014) 3002.
[58] C. Hou et al., Adv. Mater. 26 (29) (2014) 5018.
[59] S. Jung et al., Adv. Mater. 26 (28) (2014) 4825.
[60] C.-L. Choong, Adv. Mater. 26 (21) (2014) 3451.
[61] J. Park et al., ACS Nano 8 (5) (2014) 4689.
[62] X. Wang et al., Adv. Mater. 26 (9) (2014) 1336.
[63] B. Zhu et al., Small 10 (18) (2014) 3625.
[64] B. Su et al., Small 11 (16) (2015) 1886.
[65] T. Someya et al., PNAS 101 (27) (2004) 9966.
[66] C. Yeom et al., Adv. Mater. 27 (9) (2015) 1561.
[67] K. Takei et al., Nat. Mater. 9 (10) (2010) 821.
[68] Q. Sun et al., Adv. Mater. 26 (27) (2014) 4735.
[69] N.T. Tien et al., Adv. Mater. 26 (5) (2014) 796.
[70] D.-I. Kim et al., Sci. Rep. 3 (5) (2015) 12750.
[71] L. Persano et al., Nat. Commun. 4 (2013) 1633.
[72] A.B. Joshi et al., Mater. Sci. Eng. B 168 (1–3) (2010) 250.
[73] W. Wu, X. Wen, Z.L. Wang, Science 340 (6135) (2013) 952.
[74] C. Dagdeviren et al., Nat. Commun. 5 (2014) 4496.
[75] R. Bao et al., Adv. Funct. Mater. 25 (19) (2015) 2884.
[76] B. Wang et al., Nano Energy 32 (2017) 42.
[77] K. Parida et al., Nano Research 10 (10) (2017) 3557.
[78] X. Liao et al., ACS Appl. Mater. Interfaces 7 (3) (2015) 1602.
[79] J. Chun et al., Adv. Funct. Mater. 24 (14) (2014) 2038.
[80] X. Li et al., ACS Nano 8 (10) (2014) 10674.
[81] J. Zhong et al., ACS Nano 8 (6) (2014) 6273.
[82] Y. Zhang et al., Nano Energy 14 (2015) 30.
[83] Y. Yu et al., Nanoscale 9 (33) (2017) 11846.
[84] N.T. Tien et al., Adv. Mater. 21 (8) (2009) 910.
[85] M. Zirkl et al., Adv. Mater. 19 (7) (2007) 2241.
[86] T.Q. Trung et al., Org. Electron. 13 (4) (2012) 533.
[87] J. Lekkala et al., Procedia Eng. 5 (2010) 1438.
[88] P. Parzer, A. Sharma, A. Vogl, A. Olwal, M. Haller, in: Proceedings of the 30th Annual ACM Symposium on User Interface Software and Technology, Québec, QC, Canada, 22–25 October 2017.
[89] K. Takei et al., Adv. Healthcare Mater. 4 (4) (2015) 487.
[90] J. Jeon, H.B. Lee, Z. Bao, Adv. Mater. 25 (6) (2013) 850.
[91] T. Yokota et al., PNAS 112 (47) (2015) 14533.
[92] W.-H. Yeo et al., Adv. Mater. 25 (20) (2013) 2773.
[93] B. Yin et al., Nat. Commun. 9 (2018) 5161.
[94] A.H. Abdul Razak et al., Sensors 12 (7) (2012) 9884.
[95] Y. Lee et al., ACS Nano 12 (4) (2018) 4045.
[96] Y.K. Fuh, B.S. Wang, C.-Y. Tsai, Sci. Rep. 7 (1) (2017) 6759.
[97] F.-X. Wang et al., J. Mater. Chem. C 6 (46) (2018) 12575.
[98] F. Liu et al., Chem. Eur. J. 24 (63) (2018) 16823.
[99] J.-F. Shih et al., Appl. Phys. A 124 (2018) 799.
[100] J. Fiala et al., Biomed. Microdev. 15 (1) (2013) 73.
[101] X. Fan et al., Adv. Funct. Mater. 28 (44) (2018) 1805045.
[102] J. Hughes, F. Iida, Sensors 18 (11) (2018) 3822.
[103] S. Coyle, D. Morris, K. T. Lau, D. Diamond, N. Moyna, in: Proceedings of the IEEE Sixth International Workshop on Wearable and Implantable Body Sensor Networks, Berkeley, CA, USA, 3–5 June 2009; pp. 307.
[104] Y. Wanga, S. Ali, J. Wijekoon, R.H. Gong, A. Fernando, Sens. Actuators, A 282 (2018) 215.
[105] H. Liu, Z. Zhang, J. Gea, X. Lin, X. Ni, H. Yang, L. Yang, J. Mater. Sci. Technol. 35 (1) (2019) 176.
[106] K.H. Shelley, Anesth. Analg. 105 (2007) S31.
[107] R.B. Giesberts, V.I. Sluiter, G.J. Verkerke, Sensors 18 (7) (2018) 2079.
[108] D. Kang et al., Nature 516 (7530) (2014) 222.
[109] W. Gao et al., Nature 529 (7587) (2016) 509.
[110] X. Peng et al., J. Mater. Chem. A 6 (46) (2018) 23550.
[111] H. Wu et al., J. Mater. Chem. A 26 (41) (2018) 20277.
[112] S. Wu et al., ACS Appl. Mater. Interfaces 10 (42) (2018) 36312.
[113] W. Guo et al., Nanoscale 10 (37) (2018) 17751.
[114] https://www.abiresearch.com/press/sports-and-wellness-drive-mhealth-device-shipments (accessed: 27/03/2019).
[115] H.O. Adami et al., Eur. J. Cancer 37 (2001) 118.
[116] A. Rassi Jr. et al., Heart 95 (2009) 524.
[117] M. Chen et al., Mobile Netw. Appl. 21 (2016) 825.
[118] H. Kalantarian, N. Alshurafa, T. Le, M. Sarrafzadeh, in: IEEE Int. Conf. on Pervasive Computing and Communication Workshops (PerCom Workshops), IEEE, Piscataway, NJ, USA 2015, p. 348.
[119] M. Dehghani, R. M. Dangelico, in: IEEE Int. Conf. on Industrial Technology, IEEE, USA 2017, p. 1570.
[120] B. Sun, Z. Zhang, IEEE Sens. J. 15 (2015) 7161.
[121] V. Ahanathapillai et al., Healthc. Technol. Lett. 2 (2015) 34.
[122] P.-G. Jung et al., J. Dyn. Syst. Meas. Contr. 136 (2013) 011002.
[123] O. Amft et al., IEEE Pervasive Comput. 14 (2015) 32.
[124] J.-W. Jeong et al., Adv. Mater. 25 (47) (2013) 6839.
[125] C. Dagdeviren et al., Nat. Mater. 14 (7) (2015) 728.
[126] S. Ajami, F. Teimouri, J. Res. Med. Sci. 20 (2015) 1208.
[127] M. Esteban, A. Castaño, Environ. Int. 35 (2009) 438.
[128] E. Kantoch, P. Augustyniak, in: IEEE Conf. on Computers in Cardiology, IEEE, USA (2012), p. 325.
[129] M. Stoppa, A. Chiolerio, Sensors 14 (2014) 11957.
[130] M. Tamsin, IJSR 13 (2015) 697.
[131] E. Kantoch, P. Augustyniak, in: IEEE Conf. on Computers in Cardiology, IEEE, USA (2012), p. 325
[132] http://www.flexenable.com/blog/five-benefits-of-flexible-electronics-for-displays-and-sensors.
[133] A. Chortos, J. Liu, Z. Bao, Nat. Mater. 15 (9) (2016) 937.
[134] C.-K. Tee Benjamin et al., Science 250 (6258) (2015) 313.
[135] Y. Kim et al., Science 360 (6392) (2018) 998.
[136] T. Someya, Z. Bao, G.G. Malliaras, Nature 540 (7633) (2016) 379.
[137] B. Park et al., Adv. Mater. 28 (37) (2016) 8130.
[138] M.E. McConney et al., Adv. Funct. Mater. 19 (16) (2009) 2527.
[139] M. Asadnia et al., Sci. Rep. 6 (2016) 32955.
[140] D. Lee et al., Adv. Mater. 28 (42) (2016) 9364.
[141] G.Y. Bae et al., Adv. Mater. 28 (26) (2016) 5300.

[142] U. Zschieschang et al., Adv. Mater. 15 (14) (2003) 1147.
[143] J.T. Mabeck, G.G. Malliaras, Anal. Bioanal. Chem. 384 (2006) 343.
[144] V. Dua et al., Angew. Chem. Int. Ed. 49 (12) (2010) 2154.
[145] B. Crone et al., Appl. Phys. Lett. 78 (2001) 2229.
[146] Y. Noguchi, T. Sekitani, T. Someya, Appl. Phys. Lett. 89 (2006) 253507.
[147] M.F. Mabrook, C. Pearson, M.C. Petty, IEEE Sensors J. 6 (2006) 1435.
[148] J.B. Chang et al., J. Appl. Phys. 100 (2006) 014506.
[149] S. Mandal, Y.-Y. Noh, Semicond. Sci. Technol. 30 (2015) 064003.
[150] F. Liao, C. Chen, V. Subramanian, Sens. Actuators, B: Chem. 107 (2005) 849.
[151] X. Xiao et al., Adv. Mater. 23 (45) (2011) 5440.
[152] N.-K. Chang, C.-C. Su, S.-H. Chang, Appl. Phys. Lett. 92 (2008) 063501.
[153] S. Park, M. Vosguerichian, Z. Bao, Nanoscale 5 (5) (2013) 1727.
[154] Y.J. Choi et al., Nanotechnology 19 (2008) 095508.
[155] K. Parikh et al., Sens. Actuators, B: Chem. 113 (2006) 55.
[156] P.-G. Su et al., Sens. Actuators, B: Chem. 139 (2009) 488.
[157] Q. He et al., Small 8 (19) (2012) 2994.
[158] H.-C. Yuan et al., Appl. Phys. Lett. 94 (2009) 013102.
[159] A.S.G. Reddy et al., Procedia Eng. 25 (2011) 120.
[160] S. Khan, S. Tinku, L. Lorenzelli, R.S. Dahiya, IEEE Sensors J. 15 (6) (2015) 3146.
[161] G. Ashebir et al., Microelectron. Eng. 162 (2016) 6.
[162] S. Amendola et al., IEEE Trans. Microwave Theory Tech. 66 (3) (2018) 1561.
[163] C.P. Lin et al., IEEE Antennas Wirel. Propag. Lett. 10 (2011) 1108.
[164] T. Tsujimura et al., J. Soc. Inf. Display 22 (8) (2014) 412.
[165] M. Montanino et al., eXPRESS Polym. Lett. 11 (6) (2017) 518.
[166] S. Tekoglu et al., Org. Electron. 14 (2013) 3493.
[167] T. Furukawa, M. Koden, IEICE Trans. Electron. 100-C (2017) 949.
[168] L. Zhou et al., Adv. Funct. Mater. 28 (11) (2018) 1705955.
[169] M. Ye, X. Hong, X.-Y. Liu, J. Mater. Chem. A 4 (18) (2016) 6755.
[170] T. Sekine et al., Jpn. J. Appl. Phys. 55 (10S) (2016) 10TA18.
[171] G. Qian et al., Adv. Mater. 30 (12) (2018) e1704947.
[172] S. Verma et al., Appl. Mater. Today 13 (2018) 83.
[173] Y. Qin et al., Mater. Lett. 176 (2016) 68.
[174] P. Sjöberg et al., Sens. Actuators, B: Chem. 224 (2016) 325.
[175] Y. Qin et al., Adv. Funct. Mater. 26 (27) (2016) 4923.
[176] J. Arrese et al., J. Appl. Phys. 121 (2017) 104904.
[177] A.A. Chlaihawi et al., Sens. Bio-Sens. Res. 20 (2018) 9.
[178] F. Gîder et al., Angew. Chem. Int. Ed. 55 (19) (2016) 5727.
[179] M.A. Darabi et al., Adv. Mater. 29 (2017) 1700533.
[180] T. Sekine et al., Sci. Rep. 8 (2018) 4442.
[181] A. Aliane et al., Microelectron. J. 45 (2014) 1621.
[182] S. Agarwala et al., ACS Sens. 4 (1) (2019) 218–226.
[183] K. Suganuma, Introduction to Printed Electronics, 74 ed., Springer, New York, 2014, pp. 1–22.
[184] L.-M. Senentxu, M.C. Carlos, Printed Batteries: Materials, Technologies and Applications, John Wiley & Sons, Hoboken, NJ, 2018.
[185] R.R. Søndergaard et al., J. Polym. Sci. Part B: Polym. Phys. 51 (2013) 16.
[186] D. Tobjörk, R. Österbacka, Adv. Mater. 23 (17) (2011) 1935.
[187] F.C. Krebs et al., Solar Energy Mater. Solar Cells 93 (2009) 422.
[188] R. Turunen, D. Numakura, M. Nakayama, H. Kawasaki, IPC Print. Circuit Expo/APEX (2008).
[189] Y.J. Kwack, W.S. Choi, J. Korean, Physiol. Soc. 59 (2011) 3410.
[190] W.Y. Chang, T.H. Fang, S.H. Yeh, Y.C. Lin, Sensors 9 (2009) 1188.
[191] D. Novaković, N. Kašiković, G. Vladić, M. Pál, 15 – Screen printing, in: J. Izdebska, S. Thomas (Eds.), Printing on Polymers, William Andrew Publishing, 2016, pp. 247–261.
[192] R.H. Leach, R.J. Pierce, E.P. Hickman, M.J. Mackenzie, H.G. Smith, The printing ink manual, 5th ed., Springer, Netherlands, Dordrecht, the Netherlands, 1993.
[193] S. Scherp, S. J. D. Ericsson, US Patent 1981, US4267773.
[194] D.A. Clark, Major Trends in gravure printed electronics [Thesis], California Polytechnic State Univ., 2010.
[195] H. Lievens, Surf. Coat. Technol. 76 (1995) 744.
[196] B. Kang, W.H. Lee, K. Cho, ACS Appl. Mater. Interfaces 5 (7) (2013) 2302.
[197] A. Goldschmidt, H.-J. Streitburger, BASF Handbook onBasics of Coating Technology, William Andrew, Hannover, Germany, 2003.
[198] J.A. Owczarek, F.L. Howland, IEEE Trans. Compon. Packag. Manuf. Technol. 13 (1990) 358.
[199] Z. Żołek-Tryznowska, 6 - Rheology of printing inks, in: J. Izdebska, S. Thomas (Eds.), Printing on Polymers, William Andrew Publishing, 2016, p. 87.
[200] P. De Gennes, F. Brochard-Wyart, D. Quéré, Capillarity: deformable interfaces, in: Capillarity and Wetting Phenomena: Drops, Bubbles, Pearls, Waves, Springer Science and Business Media, Inc., New York, USA, 2004, pp. 2–3.
[201] K. Grundke, Characterization of polymer surfaces by wetting and electrokinetic measurements – Contact angle, interfacial tension, zeta potential, in: M. Stamm (Ed.), Polymer Surfaces and Interfaces, Springer, Berlin Heidelberg, Heidelberg, 2008, p. 103.
[202] D. Tobjörk et al., Thin Solid Films 520 (7) (2012) 2949.
[203] E. Halonen et al., IEEE Trans. Compon. Packag. Manuf. Technol. 3 (2) (2013) 350.
[204] J. Niittynen et al., Thin Solid Films 556 (2014) 452.
[205] C. Phillips et al., J. Mater. Sci. 52 (6) (2017) 9520.
[206] W. Yang et al., Adv. Mater. Technol. 3 (2) (2018) 1700241.
[207] S. Harada et al., ACS Nano 8 (12) (2014) 12851.
[208] B. Derby, Annu. Rev. Mater. Res. 40 (2010) 395.
[209] Z.P. Yin et al., Chin. Sci. Bull. 55 (30) (2010) 3383.
[210] P.F. Moonen, I. Yakimets, J. Huskens, Adv. Mater. 24 (41) (2012) 5526.
[211] B. Kim et al., Nano Lett. 14 (6) (2014) 3683.
[212] D. Stuwe et al., Adv. Mater. 27 (4) (2015) 599.
[213] Y. Sun et al., RSC Adv. 3 (30) (2013) 11925.
[214] J. Song, H. Zeng, Angew. Chem. Int. Ed. 54 (34) (2015) 9760.
[215] B.H. Kim et al., Nano Lett. 15 (2) (2015) 969.
[216] Y.S. Rim et al., Adv. Mater. 28 (22) (2016) 4415.
[217] R.G. Scalisi et al., Organic Electronics 18 (2015) 89.
[218] R. McCann et al., J. Phys. D Appl. Phys. 50 (24) (2017).
[219] C. Hughes et al., Opt. Laser Technol. 106 (2018) 265.
[220] K. Bagga et al., J. Colloid Interface Sci. 447 (2015) 263.
[221] G. Cummins, M.P. Desmulliez, Circuit World 38 (2012) 193.
[222] S. Kim et al., IEEE Microwave Mag. 14 (2013) 66.
[223] M. Gao, L. Li, Y. Song, J. Mater. Chem. C 5 (12) (2017) 2971.
[224] J. Wu et al., Lab Chip 15 (3) (2015) 690.
[225] C.-H. Choi et al., ECS J. Solid State Sci. Technol. 4 (2015) P3044.
[226] Inkjet technology for digital fabrication, ed. I.M. Hutchings, G.D. Martin, John Wiley & Sons, Ltd, Chichester, UK, 2012, p. 390.
[227] M. Singh et al., Adv. Mater. 22 (6) (2010) 673.
[228] J. Wang et al., J. Mater. Chem. C 1 (38) (2013) 6048.
[229] Y. Huang et al., Small 13 (4) (2017) 1503339.
[230] J. Sun et al., ACS Appl. Mater. Interfaces 7 (51) (2015) 28086.
[231] M. Kuang, L. Wang, Y. Song, Adv. Mater. 26 (40) (2014) 6950.
[232] D. Tian, Y. Song, L. Jiang, Chem. Soc. Rev. 42 (12) (2013) 5184.
[233] L. Wu et al., Adv. Opt. Mater. 4 (2) (2016) 1915.
[234] B.J. DeGans, P. Duineveld, U. Schubert, Adv. Mater. 16 (3) (2004) 203.
[235] H.M. Dong, W.W. Carr, J.F. Morris, Phys. Fluids 18 (2006) 072102.
[236] T.H.J.V. Osch et al., Adv. Mater. 20 (2) (2008) 343.
[237] J.C. Pita, W. Baxter, Future, opportunities and challenges of inkjet technologies, Atomization and Sprays, 2013, p. 1.
[238] P.F. Blazdell, J.R.G. Evans, J. Mater. Process. Technol. 99 (2000) 94.
[239] J.F. Mei et al., IEEE Trans. Electron. Packag. Manuf. 28 (3) (2005) 265.
[240] A.A. Halhouli et al., Sens. Rev. 38 (4) (2018) 438.
[241] B. Derby, N. Reis, MRS Bull. 28 (2003) 815.
[242] G.K. Batchelor, An Introduction to Fluid Dynamics, Cambridge University Press, 1967.
[243] N. Reis, B. Derby, M.R.S. Symp, Proc. 624 (2000) 65.
[244] O. Reynolds, Philos. Trans. R. Soc. 174 (1883) 935.
[245] V. Bergeron et al., Nature 405 (6788) (2000) 772.
[246] G.H. McKinley, M. Renardy, Phys. Fluids 23 (2011) 127101.
[247] J.E. Fromm, IBM J. Res. Dev. 28 (1984) 322.
[248] N. Reis, B. Derby, Mater. Res. Soc. Symp. Proc. 625 (2000) 117.
[249] D. Jang, D. Kim, J. Moon, Langmuir 25 (5) (2009) 2629.
[250] P. Shin, J. Sung, M.H. Lee, Microelectron. Reliab. 51 (4) (2011) 797.
[251] B. de Gans et al., Macromol. Rapid Commun. 25 (1) (2004) 292.
[252] S. Jung, I.M. Hutchings, Soft Matter 8 (2012) 2686.
[253] W.K. Hsiao et al., J. Imaging Sci. Technol. 53 (2009) 050304.
[254] F. Torrisi et al., ACS Nano 6 (4) (2012) 2992.
[255] P.G. De Gennes, Rev. Mod. Phys. 57 (1985) 827.
[256] E.G. Shafrin, W.A. Zisman, J. Phys. Chem. 64 (1960) 519.
[257] J. Israelachvili, Intermolecular and Surface Forces, Academic Press, New York, 1991.
[258] Fluid Properties Effects on Ink-Jet Device Performance, MicroFab technote 1999, online access: http://www.microfab.com/images/pdfs/technote99-02.pdf.
[259] D.E. Bugner, A.D. Bermel, IS&T NIP13: 1997 Int. Conf. on Digital Printing Technologies, Society for Imaging Science and Technology, Springfield, MA 1997, 13, p. 667.
[260] R.D. Deegan et al., Nature 389 (24) (1997) 827.

[261] A. Kamyshny, S. Magdassi, in: Inkjet-Based Micromanufacturing, (Eds: J.P. Korvink , P.J. Smith , D.-Y.Shin), Wiley-VCH, Weinheim, Germany 2012, p. 173.
[262] S. Magdassi, The Chemistry of Inkjet Inks, (Ed: S. Magdassi), World Scientific, Singapore 2010, 19.
[263] P.C. Duineveld, J. Fluid Mech. 477 (2003) 175.
[264] A.C. Arias et al., Chem. Rev. 110 (1) (2010) 3.
[265] C. Ruiz et al., J. Phys. Chem. Lett. 3 (11) (2012) 1428.
[266] C. Wang et al., Chem. Soc. Rev. 42 (7) (2013) 2592.
[267] K. Kordás et al., Small 2 (8–9) (2006) 1021.
[268] H. Okimoto et al., Adv. Mater. 22 (36) (2010) 3981.
[269] T. Takenobu et al., Appl. Phys. Express 2 (2009) 025005.
[270] A.L. Dearden et al., Macromol. Rapid Commun. 26 (2005) 315.
[271] S. Gamerith et al., Adv. Funct. Mater. 17 (16) (2007) 3111.
[272] N. Luechinger, A.E.K. Athanassiou, W.J. Stark, Nanotechnology 19 (44) (2008) 445201.
[273] B.K. Park et al., Thin Solid Films 515 (19) (2007) 7706.
[274] https://www.novacentrix.com/ (accessed: 27/03/2019)
[275] J. Li et al., Adv. Mater. 25 (29) (2013) 3985.
[276] D.J. Finn et al., J. Mater. Chem. C 2 (5) (2014) 925.
[277] K. Arapov et al., Faraday Discuss 173 (2014) 323.
[278] Y. Gao et al., Ind. Eng. Chem. Res. 53 (2014) 16777.
[279] A. Capasso et al., Solid State Commun. 224 (2015) 53.
[280] C.-L. Lee, C.-H. Chen, C.-W. Chen, Chem. Eng. J. 230 (2013) 296.
[281] S. Wang et al., Nano Lett. 10 (1) (2010) 92.
[282] L. Huang et al., Nano Res. 4 (7) (2011) 675.
[283] Y.M. Jo et al., Chem. Lett. 40 (2011) 54.
[284] L.T. Le et al., Electrochem. Commun. 13 (2011) 355.
[285] K.Y. Shin, J.-Y. Hong, J. Jang, Adv. Mater. 23 (18) (2011) 2113.
[286] K.Y. Shin, J.-Y. Hong, J. Jang, Chem. Commun. 47 (30) (2011) 8527.
[287] D. Kong et al., Langmuir 28 (37) (2012) 13467.
[288] F.J. Tölle, M. Fabritious, R. Mülhaupt, Adv. Funct. Mater. 22 (6) (2012) 1136.
[289] H. Zhang et al., Phys. Chem. Chem. Phys. 14 (37) (2012) 12757.
[290] Y. Su et al., Nano Res. 6 (11) (2013) 842.
[291] Y. Su et al., Nano Res. 8 (12) (2015) 3954.
[292] Y. Yoon et al., Sci. Rep. 5 (2015) 14177.
[293] W. Zhang et al., Colloids Surf. A 490 (2016) 232.
[294] V. Dua et al., Angew. Chem. Int. Ed. 49 (12) (2010) 2154.
[295] D.C. Han et al., J. Sens. Sci. Technol. 26 (2017) 301.
[296] F. Molina-Lopez et al., J. Micromech. Microeng. 23 (2013) 025012.
[297] M. Hösel et al., Adv. Eng. Mater. 15 (10) (2013) 995.
[298] A. Goldschmidt, H.-J. Streitberger, A. Goldschmidt, BASF handbook on basics of coating technology, 2nd ed., Vincentz Network, Hannover, Germany, 2007, p. 792.
[299] M. Lahti, S. Leppävuori, V. Lantto, Appl. Surf. Sci. 142 (1999) 367.
[300] H.A.D. Nguyen et al., IEEE Trans. Compon. Packag. Manuf. Technol. 5 (2015) 1516.
[301] H. Kang et al., Org. Electron. 15 (2014) 3639.
[302] M. Välimäki et al., Nanoscale 7 (21) (2015) 9570.
[303] P. Apilo et al., Prog. Photovolt. Res. Appl. 23 (2015) 918.
[304] M. Vilkman et al., Org. Electron. 20 (2015) 8.
[305] Y. Lin et al., Sens. Actuators B, Chem. 216 (2015) 176.
[306] D. Sung et al., IEEE Trans. Compon. Packag. Technol. 33 (2010) 105.
[307] H. Kang et al., Adv. Mater. 24 (22) (2012) 3065.
[308] R. Kitsomboonloha et al., Langmuir 28 (48) (2012) 16711.
[309] S. Kim, H.J. Sung, J. Micromech. Microeng. 25 (2015) 045004.
[310] J. Park et al., Curr. Appl. Phys. 15 (3) (2015) 367.
[311] H.A.D. Nguyen et al., J. Micromech. Microeng. 23 (2013) 095010.
[312] H.A.D. Nguyen, K.-H. Shin, D. Lee, Jpn. J. Appl. Phys. 53 (5S3) (2014) 05HC04.
[313] J. Jo et al., Jpn. J. Appl. Phys. 48 (4S) (2009) 04C181.
[314] E.B. Secor et al., Adv. Mater. 26 (26) (2014) 4533.
[315] M. Bariya et al., ACS Nano 12 (7) (2018) 6978.
[316] J.D. Park, S. Lim, H. Kim, Thin Solid Films 586 (2015) 70.
[317] W.J. Scheideler et al., J. Mater. Chem. C 4 (15) (2016) 3248.
[318] P.H. Lau et al., Nano Lett. 13 (8) (2013) 3864.
[319] W. Lee et al., Sci. Rep. 5 (2015) 17707.
[320] Q. Huang, Y. Zhu, Sci. Rep. 8 (2018) 15167.
[321] H. Kippan, Handbook of Print Media ISBN: 3-540-67326-1, Springer-Verlag, 2001.
[322] D. Deganello, J.A. Cherry, D.T. Gethin, T.C. Claypole, Thin Solid Films 520 (6) (2012) 2233.
[323] R. Leach, R. Pierce, The Printing Ink Manual, Kluwer Academic Publishers, Dordrecht, 1999.
[324] G. Hu et al., Chem. Soc. Rev. 47 (2018) 3265.
[325] F.C. Krebs, Sol. Energy Mater. Sol. Cells 93 (4) (2009) 394.
[326] B. Thompson, Printing Materials: Science and Technology, Pira International, Leatherhead, UK, 1998.
[327] R.C. Thompson, Surf. Coat. Int. Part A 1 (2001) 24.
[328] W. Heather, Printing Ink Technology and Manufacture, s.l., X-Polymers-E-Printing inks.
[329] E.W. Flick, Printing Ink and Overprint Varnish Formulations, 2nd ed., William Andrew, Norwich, US, 1999, p. 127.
[330] A.A. Tracton, Coatings Technology Handbook, 3rd ed., CRC Press, Boca Raton, US, 2005, p. 936.
[331] I.M. Hutchings, G.D. Martin, Inkjet Technology for Digital Fabrication, John Wiley & Sons, Ltd, Chichester, UK, 2012, p. 390.
[332] T. Smith, Pigm. Resin Technol. 15 (1986) 11.
[333] H. Kipphan, Handbook of Print Media: Technologies and Production Methods, 1st ed., Springer-Verlag, Berlin Heidelberg, Heidelberg, Germany, 2001, p. 1207.
[334] E.A.R.-Nastrucci, R.A. Ramirez, T.M. Weller, in: IEEE 19th Wireless and Microwave Technology Conference, WAMICON 2018, p. 1.
[335] D. Hawatmeh, T. Weller, IEEE MTT-S Int. Microwave Symp. Digest (2018) 67.
[336] G.T. Carranza et al., IEEE Trans. Compon. Packag. Manuf. Technol. (2019) 1.
[337] M. Mirotznik et al., IEEE Int. Symp. Antennas Propag. Natl. Radio Sci. Meet. (2018) 1883.
[338] A. Shen et al., IEEE Sens. J. 18 (2018) 9105.
[339] A. Shen et al., J. Magn. Magn. Mater. 46 (2018) 220.
[340] W. Jiang et al., IEEE MTT-S Int. Wirel. Symp. Proc. (2018) 3.
[341] L. Basiricó, Inkjet Printing of Organic Transistor Devices [thesis], University of Cagliari, 2012.
[342] Z. Cui, Printed Electronics: Materials, Technologies and Applications, JohnWiley & Sons Singapore Pte Ltd, Singapore, 2016, p. 360.
[343] K. Suganuma, Introduction to Printed Electronics, 74 ed., Springer, New York, US, 2014, p. 132.
[344] R.C.T. Howe et al., SPIE Nanosci. Eng. (2015) 95530R.
[345] F. Bonaccorso et al., Adv. Mater. 28 (29) (2016) 6136.
[346] F. Withers et al., Nano Lett. 14 (7) (2014) 3987.
[347] A.G. Kelly et al., Science 356 (6333) (2017) 69.
[348] D. McManus et al., Nat. Nanotechnol. 12 (24) (2017) 343.
[349] G. Hu et al., Nat. Commun. 8 (2017) 278.
[350] V. Bianchi et al., Nat. Commun. 8 (2017) 15763.
[351] Y. Xu et al., Adv. Energy Mater. 3 (8) (2013) 1035.
[352] W.J. Hyun et al., Adv. Mater. 27 (1) (2015) 109.
[353] K. Arapov et al., Adv. Funct. Mater. 26 (4) (2016) 586.
[354] P.G. Karagiannidis et al., ACS Nano 11 (3) (2017) 2742.
[355] J. Baker et al., Mater. Res. Innov. 18 (2) (2014) 86.
[356] New graphene based inks for high-speed manufacturing of printed electronics, University of Cambridge. Available at: https://www.cam.ac.uk/research/news/new-graphene-based-inks-for-high-speed-manufacturing-of-printed-electronics (accessed: 27/03/2019)
[357] E.B. Secor et al., J. Phys. Chem. Lett. 4 (8) (2013) 1347.
[358] New graphene based inks for high-speed manufacturing of printed electronics, University of Cambridge. Available at: http://www.cam.ac.uk/research/news/new-graphene-basedinks-for-high-speed-manufacturing-of-printed-electronics (accessed: 27/03/2019).
[359] S. Santra et al., Sci. Rep. 5 (2015) 17374.
[360] E.B. Secor et al., Chem. Mater. 29 (5) (2017) 2332.
[361] T. Carey et al., Nat. Commun. 8 (2017) 1202.
[362] D.D. Arhin et al., Carbon 105 (2016) 33.
[363] D.B.R. Kumar et al., Eur. Polym. J. 36 (2000) 1503.
[364] S. Merilampi et al., Microelectron. Reliab. 50 (12) (2010) 2001.
[365] A.J. Bandodkar et al., Adv. Mater. 27 (19) (2015) 3060.
[366] M. Hu et al., ACS Nano. 10 (1) (2016) 396.
[367] N. Matsuhisa et al., Nat. Commun. 6 (2015) 8461.
[368] R. Ma et al., ACS Nano 9 (11) (2015) 10876.
[369] D.R. Karsa, Surfactants in Polymers, Coatings, Inks and Adhesives, Vol. 1, Taylor & Francis, UK, 2003.
[370] D. Jang et al., Adv. Funct. Mater. 18 (19) (2008) 2862.
[371] S.B. Walker, J.A. Lewis, J. Am. Chem. Soc. 134 (3) (2012) 1419.
[372] J.K. Fink, The Chemistry of Printing Inks and Their Electronics and Medical Applications, John Wiley & Sons, Hoboken, 2014.
[373] A. Kamyshny, J. Steinke, S. Magdassi, Open Appl. Phys. J. 4 (2011) 19.
[374] B.I. Yakobson, C.J. Brabec, J. Bernholc, Phys. Rev. Lett. 76 (1996) 2511.
[375] M.M.J. Treacy, T.W. Ebbesen, J.M. Gibson, Nature 381 (1996) 678.
[376] E.W. Wong, P.E. Sheehan, C.M. Lieber, Science 277 (1997) 1971.

[377] P. Lee et al., Adv. Mater. 24 (25) (2012) 3326.
[378] X. Shuai et al., ACS Appl. Mater. Interfaces 9 (31) (2017) 26314.
[379] W. Huang et al., ACS Appl. Mater. Interfaces 9 (48) (2017) 42266.
[380] M. Jian et al., Adv. Funct. Mater. 27 (9) (2017) 1606066.
[381] L. Nela et al., Nano Lett. 18 (3) (2018) 2054.
[382] S.-J. Park et al., Adv. Mater. Technol. 3 (1) (2018) 1700158.
[383] C. Zhu et al., Nano Lett. 16 (6) (2016) 3448.
[384] J.H. Chen et al., Adv. Mater. 19 (21) (2007) 3623.
[385] Y. Hu et al., J. Mater. Chem. C. 4 (24) (2016) 5839.
[386] E. Skotadis et al., Sens. Actuators B. 189 (2013) 106.
[387] X. Wang et al., Adv. Mater. 27 (15) (2015) 2324.
[388] V.C. Maheshwari, R. Saraf, Science 312 (5779) (2006) 1501.
[389] T.S. Sreeprasad et al., Nano Lett. 13 (4) (2013) 1757.
[390] A. Tang et al., Carbohydr. Polym. 148 (2016) 29.
[391] V. Wood et al., Adv. Mater. 21 (21) (2009) 2151.
[392] X. Cao et al., ACS Nano. 8 12 (2014) 12769.
[393] G. Pangalos, J.M. Dealy, M.B. Lyne, J. Rheol. 29 (1985) 471.
[394] D. Doraiswamy, Rheol. Bull. 71 (2002) 1.
[395] H.A. Barnes, J.F.J.F. Hutton, K. Walters, An Introduction to Rheology, 1st ed., Elsevier, Amsterdam, The Netherlands, 1989, p. 199.
[396] Z. Żołek-Tryznowska, 6 - Rheology of printing inks, in: J. Izdebska, S. Thomas (ed.), Printing on Polymers, William Andrew Publishing, 2016, p. 87.
[397] R.P. Ortiz, A. Facchetti, T.J. Marks, Chem. Rev. 110 (2010) 205.
[398] G. Vescio et al., J. Mater. Chem. C 4 (9) (2016) 1804.
[399] L. Liu, Y.P. Feng, Z.X. Shen, Phys. Rev. B 68 (2003) 104102.
[400] I. Jo et al., Nano Lett. 13 (2) (2013) 550.
[401] C.R. Dean et al., Nat. Nanotechnol. 5 (10) (2010) 722.
[402] F. Hui et al., Microelectron. Eng. 163 (2016) 119.
[403] L.H. Li et al., Nano Lett. 15 (1) (2015) 218.
[404] A.K. Geim, I.V. Grigorieva, Nature 499 (7459) (2013) 419.
[405] Y. Hernandez et al., Nat. Nanotechnol. 3 (9) (2008) 563.
[406] G.-H. Lee et al., Appl. Phys. Lett. 99 (2011) 243114.
[407] M. Osada, T. Sasaki, Adv. Mater. 24 (2) (2012) 210.
[408] R.V. Gorbachev et al., Small 7 (4) (2011) 465.
[409] L. Britnell et al., Nano Lett. 12 (3) (2012) 1707.
[410] T.M. Schmidt et al., Adv. Energy Mater. 5 (15) (2015) 1500569.
[411] H. Lu et al., Appl. Phys. Lett. 106 (2015) 093302.
[412] J. Doggart, Y. Wu, S. Zhu, Appl. Phys. Lett. 94 (16) (2009) 163503.
[413] B.S. Ong et al., J. Am. Chem. Soc. 126 (11) (2004) 3378.
[414] A.C. Arias et al., Appl. Phys. Lett. 85 (15) (2004) 3304.
[415] Y. Wu et al., Appl. Phys. Lett. 86 (14) (2005) 142102.
[416] N.D. Treat et al., Nat. Mater. 12 (7) (2013) 628.
[417] J. Kwon et al., Adv. Sci. 3 (5) (2016) 1500439.
[418] J. Lee et al., Adv. Mater. 25 (41) (2013) 5886.
[419] M.M. Rehman et al., Sci. Rep. 6 (2016) 36195.
[420] A. Kim et al., ACS Nano 7 (2) (2013) 1081.
[421] X. Lin et al., Adv. Sci. 2 (6) (2015) 1500028.
[422] K. Bagga et al., RSC Advances 7 (13) (2017) 8060.
[423] J.S. Gebauer et al., J. Colloid Interface Sci. 526 (2018) 400.
[424] J.J. Schneider et al., J. Mater. Chem. 19 (10) (2009) 1449.
[425] S.Y. Cui et al., J. Mater. Chem. C 4 (26) (2016) 6371.
[426] L. Sooman et al., Nanotechnology 27 (43) (2016) 435501.
[427] S.J. Rowley-Neale et al., Sustainable Energy Fuels 1 (2017) 74.
[428] D. Madan et al., ACS Appl. Mater. Interfaces 4 (11) (2012) 6117.
[429] V. Forsberg et al., J. Imaging Sci. 60 (2016) 40405.
[430] E.B. Secor, M.C. Hersam, J. Phys. Chem. Lett. 6 (2015) 620.
[431] J. Li et al., Adv. Funct. Mater. 24 (41) (2014) 6524.
[432] Y. Sun, J.A. Rogers, Adv. Mater. 19 (15) (2007) 1897.
[433] Y. Sun, Y. Xia, Science 298 (5601) (2002) 2176.
[434] B. Wiley, Y. Sun, Y. Xia, Acc. Chem. Res. 40 (10) (2007) 1067.
[435] M. Yamamoto, Y. Kashiwagi, M. Nakamoto, Langmuir 22 (20) (2006) 8581.
[436] A. Pyatenko, M. Yamaguchi, M. Suzuki, J. Phys. Chem. C 111 (2007) 7910.
[437] T. Kraus et al., Nat. Nanotechnol. 2 (9) (2007) 570.
[438] D. Feng et al., Chem. Commun. 47 (2011) 8557.
[439] M. Amjadi et al., ACS Nano 8 (5) (2014) 5154.
[440] S. Hong et al., Adv. Mater. 27 (32) (2015) 4744.
[441] D. Son et al., ACS Nano 9 (5) (2015) 5585.
[442] L.F. Ma et al., Compos. Sci. Technol. 128 (2016) 176.
[443] X. Wang, J. Sparkman, J. Gou, Compos. Commun. 3 (2017) 1.
[444] Y. Liu et al., Composites A 80 (2016) 95.
[445] C. Bonavolontàa et al., Sens. Actuators A 252 (2016) 26.
[446] J. Ren et al., Carbon 111 (2017) 622.
[447] Y. Abdul Samad et al., Sens. Actuators B 240 (2017) 1083.
[448] B.Y. Ahn et al., Science 323 (5921) (2009) 1590.
[449] T. Sekitani et al., Nat. Mater. 8 (6) (2009) 494.
[450] T. Araki et al., IEEE Electron Device Lett. 32 (10) (2011) 1424.
[451] K.-Y. Chun et al., Nat. Nanotechnol. 5 (12) (2010) 853.
[452] M. Park et al., Nat. Nanotechnol. 7 (12) (2012) 803.
[453] Z. Tehrani et al., Org. Electron. 26 (2015) 386.
[454] S. Lehtimaki et al., Electr Power Energy Syst 58 (2014) 42.
[455] Z. Tehrani et al., Energy 118 (2017) 1313.
[456] I. Svancara et al., Electroanalysis 21 (1) (2009) 7.
[457] P.L. Cheng et al., IEEE Trans. Compon. Packag. Technol. 30 (2) (2007) 269.
[458] N. Serra et al., Procedia Chem. 1 (1) (2009) 48.
[459] L. Zhang et al., J. Mater. Chem. A 3 (17) (2015) 9165.
[460] D. Janczak et al., Sensors 14 (9) (2014) 17304.
[461] S. Wang et al., RSC Adv. 5 (104) (2015) 85799.
[462] S.X. Wu et al., Small 9 (8) (2013) 1160.
[463] T. Xie et al., Ceram. Int. 45 (2019) 2516.
[464] L. Zhao, B. Jiang, Y. Huang, J. Mater. Sci. 54 (2019) 5472.
[465] C.H. Xu et al., Energy Environ Sci. 6 (5) (2013) 1388.
[466] Y. Chen et al., Phys. Chem. Phys. 15 (23) (2013) 9170.
[467] G.-H. Lee et al., Science 340 (6136) (2013) 1073.
[468] L.Z. Feng, Z.A. Liu, Nanomedicine (Lond.) 6 (2011) 317.
[469] G. Goncalves, Adv. Healthc Mater. 2 (8) (2013) 1072.
[470] Y. Wang et al., Small 10 (1) (2014) 109.
[471] J.J. Castillo et al., Analyst. 138 (4) (2013) 1026.
[472] J.Y. Chen et al., Int. J. Electrochem. Sci. 8 (2013) 3963.
[473] C. Hu et al., ACS Appl. Mater. Interfaces 5 (11) (2011) 4760.
[474] O.S. Kwon et al., Adv. Mater. 25 (30) (2013) 4177.
[475] X.D. Wang et al., J. Biosens Bioelectron. 47 (2013) 171.
[476] K.P. Liu et al., J. Mater. Chem. 21 (32) (2011) 12034.
[477] Y.Z. Pan, N.G. Sahoo, L. Li, Expert Opin. Drug. Deliv. 9 (11) (2012) 1365.
[478] H. Shen et al., Theranostics 2 (2012) 283.
[479] X.S. Zhuang et al., Nano Res. 1 (3) (2008) 203.
[480] K. Yang et al., Nano Lett. 10 (9) (2010) 3318.
[481] R.R. Nair et al., Science 320 (5881) (2008) 1308.
[482] J.W. Suk et al., Nano Lett. 13 (4) (2013) 1462.
[483] F. Liu, P.M. Ming, J. Li, Phys Rev B. 76 (2007) 064120.
[484] A.A. Balandin, Nat Mater. 10 (8) (2011) 569.
[485] C. Lee et al., Science 321 (5887) (2008) 385.
[486] K.P. Loh et al., J. Mater. Chem. 20 (12) (2010) 2277.
[487] J.S. Bunch et al., Nano Lett. 8 (8) (2008) 2458.
[488] S. Eigler, A. Hirsch, Angew. Chem., Int. Ed. 53 (30) (2014) 7720.
[489] D.R. Dreyer et al., Chem. Soc. Rev. 39 (2010) 228.
[490] M.J. Allen, V.C. Tung, R.B. Kaner, Chem. Rev. 110 (1) (2010) 132.
[491] S. Park, R.S. Ruoff, Nat. Nanotechnol. 4 (4) (2009) 217.
[492] Y. Zhu et al., Adv. Mater. 22 (35) (2010) 3906.
[493] G. Eda, M. Chhowalla, Adv. Mater. 22 (22) (2010) 2392.
[494] B.C. Brodie, Ann. Chim. Phys. 59 (1860) 466.
[495] L. Staudenmaier, Ber. Dtsch. Chem. Ges. 31 (2) (1898) 1481.
[496] C. Mattevi et al., Adv. Funct. Mater. 19 (16) (2009) 2577.
[497] W.W. Cai et al., Science 321 (5897) (2008) 1815.
[498] S. Stankovich et al., Carbon 44 (15) (2006) 3342.
[499] J.I. Paredes et al., Langmuir 24 (19) (2008) 10560.
[500] S. Borini et al., ACS Nano 7 (12) (2013) 11166.
[501] R. Guo et al., Adv. Mater. 25 (24) (2013) 3343.
[502] N.T. Furtak, E. Skrzetuska, I. Krucińska, Fibres Text. Eastern Europe 21 (2013) 84.
[503] R.D. Ponce Wong, J.D. Posner, V.J. Santos, Sens. Actuators, A: Phys. 179 (2012) 62.
[504] M.S. Bar et al., ACS Appl. Mater. Interfaces 5 (12) (2013) 5531.
[505] J. Lee et al., Nanoscale 6 (20) (2014) 11932.
[506] K. Saetia et al., Adv. Funct. Mater. 24 (4) (2014) 492.
[507] K. Black et al., Sci. Rep. 6 (2016) 20814.
[508] V. Correia et al., Smart Mater. Struct. 22 (2013) 105028.
[509] M.D. Dankoco et al., Mater. Sci. Eng. B 205 (2016) 1.
[510] B.I. Morshed et al., J. Low Power Electron. Appl. 7 (4) (2017) 26.
[511] G. Mattana et al., IEEE Sensors Journal 13 (2013) 3901.
[512] J. Courbat, Y.B. Kim, D. Briand, N.F. de Rooij, in: Actuators and Microsystems Conference (TRANSDUCERS), 2011 16th International, T3P.089.
[513] J. Ferri et al., Materials 10 (12) (2017) 1450.
[514] Z. Zhou et al., J. Mater. Chem. C 6 (48) (2018) 13120.
[515] S. Gong et al., Nat. Commun. 5 (2014) 163.
[516] T. Sekitani et al., Science 321 (5895) (2008) 1468.
[517] R. Zhang, B. Peng, Y. Yuan, Composites Sci. Technol. 168 (2018) 118.

[518] Y. Yuan et al., RSC Adv. 6 (114) (2016) 113298.
[519] S. Harada et al., ACS Nano 8 (12) (2014) 12851–12857.
[520] S. Bielska, M. Sibinski, A. Lukasik, Mater. Sci. Eng. B 165 (1–2) (2009) 50.
[521] K. Teng, R. Vest, IEEE Trans. Compon. Hybrids Manuf. Technol. 10 (1987) 545.
[522] S.F. Jahn et al., Chem. Mater. 22 (10) (2010) 3067.
[523] P. Jolke et al., Nanotechnology 20 (16) (2009) 165303.
[524] N. Komoda et al., ACS Appl. Mater. Interfaces 4 (11) (2012) 5732.
[525] M. Abulikemu et al., Angew. Chem. Int. Ed. 53 (2) (2014) 420.
[526] D. Li et al., J. Mater. Chem. 19 (22) (2009) 3719.
[527] J. Niittynen et al., Sci. Rep. 5 (2015) 8832.
[528] L. Del Carro, J. Zurcher, U. Drechsler, I. Clark, G. Ramos, T. Brunschwiler, IEEE Trans. Components, Packag. Manuf. Technol. 2019, 1.
[529] N.G. Park et al., Adv. Mater. 17 (19) (2005) 2349.
[530] J.W. Boley, E.L. White, R.K. Kramer, Adv. Mater. 27 (14) (2015) 2355.
[531] B.-G. Park, C.-J. Lee, S.-B. Jung, Microelectron. Eng. 202 (2018) 37.
[532] Y.-T. Kwon et al., ACS Appl. Mater. Interfaces 10 (50) (2018) 44071.
[533] C.E. Knapp et al., Adv. Mater. Technol. 3 (3) (2018) 1700326.
[534] E. Balliu et al., Sci. Rep. 8 (2018) 10408.
[535] S. Liu et al., ACS Appl. Mater. Interfaces 10 (33) (2018) 28232.
[536] I. Theodorakos et al., Appl. Surf. Sci. 336 (2015) 157.
[537] W. Shou et al., Adv. Mater. 29 (26) (2017) 1700172.
[538] M. Dexter et al., Sci. Rep. 8 (1) (2018) 2201.
[539] A. Kenfack et al., Livest. Res. Rural Dev. 27 (2015) 8832.
[540] S.H. Ko et al., Sens. Actuators, A: Phys. 134 (2007) 161.
[541] M. Borghetti et al., Sens. Actuators, A: Phys. 243 (2016) 71.
[542] J.Y. Lim, S.Y. Kim, Polym. J. 36 (2004) 769.
[543] J.H. Waller et al., Thin Solid Films 519 (13) (2011) 4249.
[544] S. Khan, L. Lorenzelli, R.S. Dahiya, IEEE Sens. J. 15 (6) (2015) 3164.
[545] R.D. Widdle Jr. et al., Int. J. Eng. Sci. 46 (1) (2008) 31.
[546] H.-Y. Mi et al., Mater. Des. 56 (2014) 398.
[547] N.Q. Balaban et al., Nature Cell Biol. 3 (5) (2001) 466.
[548] Y. Chan et al., Polymer 47 (2006) 5124.
[549] K. Nakamae, T. Nishino, Y. Gotoh, Polymer 36 (1995) 1401.
[550] M. Guo, H.G. Zachmann, Macromolecules 30 (1997) 2746.
[551] A. Nathan et al., Proc. IEEE 100 (2012) 1486.
[552] M.-C. Choi, Y. Kim, C.-S. Ha, Prog. Polym. Sci. 33 (2008) 581.
[553] G.P. Crawford (Ed.), Flexible Flat Panel Displays, John Wiley and Sons Ltd., 2005.
[554] https://www.azom.com/article.aspx?ArticleID=468 (accessed: 27/03/2019).
[555] http://www.matweb.com/search/DataSheet.aspx?MatGUID=60dc5dfcf5ba48f9bb4fe2fc7d7dd4bf (accessed: 27/03/2019).
[556] P.B. Kosaraju, K.K. Sirkar, J. Membr. Sci. 321 (2) (2008) 155.
[557] C. Vasile (Ed.), Handbook of Polyolefins, CRC Press, Talor and Francis Group, 2000.
[558] I.U. Ahad et al., Acta Phys. Pol. A 129 (2) (2016) 241.
[559] S. Harada et al., ACS Nano 8 (4) (2014) 3921.
[560] D. Knitiel, E. Schollmeyer, Anal. Chim. Acta 226 (2) (1989) 247.
[561] N. Luo et al., Adv. Funct. Mater. 26 (8) (2016) 1178.
[562] C. Pang et al., Nat. Mater. 11 (9) (2012) 795.
[563] J. Chen et al., Nat. Energy 1 (8) (2016) 16138.
[564] M. Hamedi, R. Forchheimer, O. Inganas, Nat. Mater. 6 (5) (2007) 357.
[565] R. Salvado et al., Sensors 12 (2012) 15841.
[566] J. Edmison, et al. Proc. Int. Workshop Wearable Implant. Body Sensors Netw. 2006, 131.
[567] G. Magenes, et al. Proc. 33rd Annu. Int. Conf. IEEE Eng. Med. Biol. Soc. 2011, 8365.
[568] M. Sibinski, M. Jakubowska, M. Sloma, Sensors 10 (2010) 7934.
[569] R. Paradiso, G. Loriga, N. Taccini, IEEE Trans. Inf. Technol. Biomed. 9 (2005) 337.
[570] J. Soyoun, J. Taeksoo, K.V. Vijay, Smart Mater. Struct. 15 (2006) 1872.
[571] S. Lee et al., Adv. Funct. Mater. 25 (21) (2015) 3105.
[572] G.H. Büscher et al., Robot. Auton. Syst. 63 (2015) 244.
[573] S. Li et al., ACS Appl. Mater. Interfaces 7 (27) (2015) 14912.
[574] E. Sardini et al., IEEE Trans. Instrum. Measur. 64 (2015) 439.
[575] O. Tirosh, R. Begg, E. Passmore, N.K. Steinberg, 2013 Seventh International Conference on Sensing Technology (ICST) New Zeland, 2013, 618.
[576] Z. Zhou et al., J. Mater. Chem. C 6 (48) (2018) 13120.
[577] Y. Wei et al., J. Mater. Chem. C 4 (5) (2016) 935.
[578] N. Matsuhisa et al., Nat. Mater. 16 (8) (2017) 834.
[579] S. Takamatsu et al., Adv. Mater. 28 (22) (2016) 4485.
[580] Z. Ma et al., Nanoscale 10 (15) (2018) 7116.
[581] M. Liu et al., Adv. Mater. 29 (41) (2017) 1703700.
[582] B. Yao et al., Adv. Sci. 4 (7) (2017) 1700107.
[583] S.Z. Hossain et al., Anal. Chem. 81 (13) (2009) 5474.
[584] Q. Zhong et al., Energy Environ. Sci. 6 (2013) 1779.
[585] X. Fan et al., ACS Nano 9 (4) (2015) 4236.
[586] S. Yun et al., Appl. Phys. Lett. 95 (2009) 104102.
[587] S. Kanaparthi, S. Badhulika, Green Chem. 18 (2016) 3640.
[588] Y. Fujisaki et al., Adv. Funct. Mater. 24 (12) (2014) 1657.
[589] R. Zhao et al., RSC Adv. 3 (45) (2013) 23178.
[590] L. Hu et al., PNAS 106 (51) (2009) 21490.
[591] A. Razaq et al., Adv. Energy Mater. 2 (4) (2012) 445.
[592] J.M. Nassar et al., Adv. Mater. Technol. 2 (4) (2017) 1600228.
[593] S. Chen, Y. Song, F. Xu, ACS Appl. Mater. Interfaces 10 (40) (2018) 34646.
[594] B.G. Choi et al., ACS Nano 5 (9) (2011) 7205.
[595] P. Maharjan, R.M. Toyabur, J.Y. Park, Nano Energy 46 (2018) 383.
[596] R. Vilkhu et al., IEEE Access 6 (2018) 28945.
[597] Y. Yang et al., Nano Res. 5 (12) (2012) 888.
[598] Y.-Y. Chiu et al., Sens. Actuators, A 189 (2013) 328.
[599] N. Wu et al., Adv. Funct. Mater. 25 (30) (2015) 4788.
[600] P.-K. Yang et al., Adv. Mater. 27 (25) (2015) 3817.
[601] K. Lahiri, S. Dey, D. Panigrahi, A. Raghunathan, in: Proc. of the Asia and South Pacific Design Automation Conference, Bangalore, India, January 2002.
[602] Z. Wang et al., Adv. Mater. 26 (6) (2014) 970.
[603] M.H. Park et al., Adv. Mater. 22 (3) (2010) 415.
[604] H. Liu et al., Adv. Funct. Mater. 25 (45) (2015) 7071.
[605] H. Gwon et al., Energy Environ. Sci. 4 (2011) 1277.
[606] A.M. Gaikwad et al., Adv. Mater. 23 (29) (2011) 3251.
[607] A.M. Gaikwad et al., Energy Technol. 1 (2–3) (2013, 2013,) 177–185.
[608] N. Li et al., Proc. Natl. Acad. Sci. USA 109 (43) (2012) 17360.
[609] Z. Pan et al., Adv. Energy Mater. 6 (11) (2016) 1600271.
[610] W. Weng et al., Adv. Mater. 27 (8) (2015) 1363.
[611] Z. Zhang et al., Adv. Energy Mater. 7 (5) (2017) 1601814.
[612] W. Liu et al., Adv. Mater. 29 (1) (2017) 1603436.
[613] Y. Gogotsi, P. Simon, Science 334 (6058) (2011) 917.
[614] Q. Cheng et al., Nano Lett. 13 (10) (2013) 4969.
[615] A.M. Zamarayeva et al., Sci. Adv. 3 (6) (2017) e1602051.
[616] L. Noerochim et al., J. Mater. Chem. 22 (22) (2012) 11159.
[617] L. Li et al., Energy Environ. Sci. 7 (2014) 2101.
[618] J.M. Tarascon, M. Armand, Nature 414 (6861) (2001) 359.
[619] I.Y. Choi et al., Angew. Chem. Int. Ed. 54 (4) (2015) 1049.
[620] G. Heo et al., Sci. Rep. 3 (6) (2016) 25358.
[621] Y. Liu et al., J. Electrochem. Soc. 159 (2012) A349.
[622] H.-J. Ha et al., Energy Environ Sci. 5 (4) (2012) 6491.
[623] G. Zhou, F. Li, H.M. Cheng, Energy Environ Sci 7 (4) (2014) 1307.
[624] Y. Zhang et al., Angew. Chem. Int. Ed. 53 (52) (2014) 14564.
[625] Y. Zhang et al., Angew. Chem. Int. Ed. 54 (38) (2015) 11177.
[626] M. Koo et al., Nano Lett. 12 (9) (2012) 4810.
[627] Z. Song et al., Nat. Commun. 5 (2014) 3140.
[628] W. Weng et al., Nano Lett. 14 (6) (2014) 3432.
[629] S. Xu et al., Nat. Commun 4 (2013) 1543.
[630] S. Leijonmarck et al., J. Mater. Chem. A 1 (15) (2013) 4671.
[631] Y. Chen et al., Chem. Eng. J. 353 (2018) 499.
[632] L. Liu et al., Adv. Mater. Technol. 3 (1) (2018) 1700206.
[633] K. Jost et al., Energy Environ. Sci. 6 (2013) 2698.
[634] L. Liu et al., J. Power Sources 397 (2018) 59.
[635] K.-H. Choi et al., Energy Environ. Sci. 9 (2016) 2812.
[636] H. Lee et al., J. Mater. Chem. 3 (16) (2015) 8339.
[637] S.S. Delekta et al., Nanoscale 9 (21) (2017) 6998.
[638] P. Sundriyal, S. Bhattacharya, ACS Appl. Mater. Interfaces 9 (44) (2017) 38507.
[639] S. Kang et al., ACS Appl. Mater. Interfaces 10 (1) (2018) 1033.
[640] C.J. Zhang et al., Nat. Commun. 10 (1795) (2019) 1–9.
[641] Y. Wang et al., Nano Energy 49 (2018) 481.
[642] L. Li et al., Adv. Energy Mater. 6 (20) (2016) 1600909.
[643] W.J. Hyun et al., Adv. Energy Mater. 7 (17) (2017) 1700285.
[644] H.W. Tan et al., Adv. Electron. Mater. 5 (5) (2019) 1800831.
[645] H.W. Tan, T. Tran, C.K. Chua, Virtual Phys. Prototyp. 11 (4) (2016) 271.
[646] N. Saengchairat, T. Tran, C.-K. Chua, Virtual Phys. Prototyp. 12 (1) (2017) 31.
[647] V. Francis, P.K. Jain, Virtual Phys. Prototyp. 12 (2) (2017) 107.
[648] L. Wang et al., Chem. Soc. Rev. 46 (2017) 6764.
[649] S. Chen et al., Adv. Mater. 30 (2018) 1705400.
[650] L. Wang et al., Adv. Mater. 31 (2019) 1804583.
[651] H. Kang et al., Sci. Rep. 4 (5387) (2014) 1.
[652] M. Xie et al., Adv. Mater. Technol. 4 (3) (2019) 1800626.
[653] I. Graz et al., Appl. Phys. Lett. 89 (2006) 073501.
[654] S. Harada et al., ACS Nano 8 (2014) 3921.

[655] D.J. Finn, M. Lotya, J.N. Coleman, ACS Appl. Mater. Interfaces 7 (17) (2015) 9254.
[656] S. Jeong et al., J. Phys. Chem. C 114 (2010) 22277.
[657] A. Kosmala et al., Mater. Chem. Phys. 129 (2011) 1075.
[658] I. Shown et al., Energy Sci. Eng. 3 (2015) 2.
[659] Y.H. Hu, X.L. Sun, J. Mater. Chem. A 2 (2014) 10712.
[660] S.Y. Lee et al., Energy Environ. Sci. 6 (2013) 2414.
[661] J. Huang et al., Thin Solid Films 516 (2008) 3314.
[662] Y. Zhao et al., J. Solid State Electrochem. 13 (2008) 705.
[663] R.E. Sousa et al., Electrochim. Acta 196 (2016) 92.
[664] M.-S. Park, S.-H. Hyun, S.-C. Nam, Electrochim. Acta 52 (2007) 7895.
[665] J. Ren et al., Adv. Mater. 25 (2013) 1155.
[666] G. Qian et al., ACS Energy Lett. 4 (2019) 690.
[667] K. Fu et al., Adv. Mater. 28 (2016) 2587.
[668] http://www.europarl.europa.eu/news/it/press-room/20131004IPR21519/meps-ban-cadmium-from-power-tool-batteries-and-mercury-from-button-cells. [Accessed: 26-Jun-2019].
[669] https://www.idtechex.com/en/research-report/non-toxic-materials-for-electronics-electrics-large-emerging-markets-2018-2028/589. [Accessed: 26-Jun-2019].
[670] C. Liao et al., Adv. Mater. 27 (46) (2015) 7493.
[671] G. Lanzani, Nat. Mater. 13 (8) (2014) 775.
[672] X. Crispin et al., Chem. Mater. 18 (18) (2006) 4354.
[673] M. Hedges, A.B. Marin, in: DDMC 2012 Conf. (2012), pp. 1–5.
[674] J. Bourassa et al., SN Appl. Sci. 1 (2019) 517.
[675] Q. Jing et al., Adv. Mater. Technol. 4 (2019) 1800328.
[676] T. Pandhi et al., Sci. Rep. 8 (2018) 10842.
[677] L.J. Deiner et al., Adv. Eng. Mater. 21 (2019) 1801281.
[678] L.J. Deiner, T.L. Reitz, Adv. Eng. Mater. 19 (2017) 1600878.
[679] D. Espalin et al., Int. J. Adv. Manuf. Technol. 72 (2014) 963.
[680] A. Hohnholz et al., J. Laser Appl. 31 (2019) 022301.